Spectropolarimetry of Supernovae

Lifan Wang[1] and J. Craig Wheeler[2]

[1]Physics Department, Texas A&M University, College Station, Texas 77843; email: wang@physics.tamu.edu

[2]Department of Astronomy, University of Texas, Austin, Texas 78712; email: wheel@astro.as.utexas.edu

Annu. Rev. Astron. Astrophys. 2008. 46:433–74

First published online as a Review in Advance on June 3, 2008

The *Annual Review of Astronomy and Astrophysics* is online at astro.annualreviews.org

This article's doi: 10.1146/annurev.astro.46.060407.145139

0066-4146/08/0922-0433$20.00

Key Words

cosmology, polarimetry, stars, stellar evolution

Abstract

Overwhelming evidence has accumulated in recent years that supernova explosions are intrinsically three-dimensional phenomena with significant departures from spherical symmetry. We review the evidence derived from spectropolarimetry that has established several key results: Virtually all supernovae are significantly aspherical near maximum light; core-collapse supernovae behave differently than thermonuclear (Type Ia) supernovae; the asphericity of core-collapse supernovae is more pronounced in the inner layers, showing that the explosion process is strongly aspherical; core-collapse supernovae tend to establish a preferred direction of asymmetry; and the asphericity is stronger in the outer layers of thermonuclear supernovae, providing constraints on the burning process. We emphasize the utility of the *Q/U* plane as a diagnostic tool and revisit SN 1987A and SN 1993J in a contemporary context. An axially symmetric geometry can explain many basic features of core-collapse supernovae, but significant departures from axial symmetry are needed to explain most events. We introduce a spectropolarimetry type to classify the range of behavior observed in polarized supernovae. Understanding asymmetries in supernovae is important for phenomena as diverse as the origins of gamma-ray bursts and the cosmological applications of Type Ia supernovae in studies of the dynamics of the universe.

1. INTRODUCTION

Supernovae have been studied with modern scientific methods for nearly a century. During this time, most scientists have assumed that these catastrophic stellar explosions are, for all practical purposes, spherically symmetric. There was no commanding observational need to abandon that simplifying assumption, until now.

This review separates supernovae into two major groups: (*a*) Type Ia supernovae and (*b*) all the other types that include, for example, Type II, Type IIb, Type Ib, and Type Ic (Harkness & Wheeler 1990, Filippenko 1997) (see Spectral Types sidebar). Evidence that supernovae may depart a little or even drastically from spherical symmetry has been growing for years. For core collapse, we know that pulsars are somehow kicked at birth in a manner that requires a departure from both spherical and up/down symmetry (Lyne & Lorimer 1994). The progenitor star of SN 1987A was asymmetric as are its surroundings and debris (Crotts, Kunkel & McCarthy 1989; Wampler et al. 1990; Burrows et al. 1995; Wang et al. 2002). The supernova remnant Cassiopeia A shows signs of a jet and counterjet that have punched holes in the expanding shell of debris, and there are numerous other asymmetric supernova remnants (Fesen 2001; Hwang et al. 2004; Wheeler, Maund & Couch 2008). Each of these observations is well-known. The question has been whether they are merely incidental or whether they offer vital clues on how core-collapse supernovae work.

For Type Ia supernovae (Hillebrandt & Niemeyer 2000), the progenitor white dwarf has long been treated as basically spherically symmetric, even though in the popular model the explosion must take place in a binary system in which the white dwarf grows to its critical mass by accretion of mass and, inevitably, angular momentum. There could be asymmetries in this kind of supernova resulting from the dynamics of the combustion process, the spin of the white dwarf, the stellar orbital motion, a surrounding accretion disk, or the presence of a companion star. As for the case of core-collapse supernovae, these possibilities were known, but there was no compelling observational reason to consider departures from spherical symmetry. This, too, is changing.

Our understanding of the shape of supernovae has been revolutionized in the past decade. The driving force has been a new type of observation: spectropolarimetry. When light scatters through the expanding debris of a supernova, it retains information about the orientation of the scattering layers. Because we cannot spatially resolve the average extragalactic supernova through direct imaging, polarization is the most powerful tool we have to judge the morphology of the ejecta. Spectropolarimetry measures both the overall shape of the emitting region and the shape of regions comprising particular chemical elements. For a supernova with a typical photospheric radius of 10^{15} cm, the effective spatial resolution attained by polarimetry at 10 Mpc is 10 μarcsec. This is a factor of 100 better resolution than optical interferometers can give us at a small fraction of their cost.

The spectropolarimetry of supernovae matured over the past decade in parallel with two other immense revolutions: the supernova/gamma-ray-burst connection and the use of Type Ia

SPECTRAL TYPES

Type II supernovae show distinct lines of hydrogen, whereas Type I supernovae do not. SN 1987A was a Type II supernova, but its progenitor was a blue supergiant rather than the more common red supergiant. Type Ia supernovae result from exploding white dwarfs, whereas Type Ib and Ic supernovae result from core collapse. The progenitors of Type IIb supernovae have a thin hydrogen envelope, $\sim$0.1 $M_{\odot}$.

supernovae to discover the acceleration of the universe. The understanding that core-collapse supernovae are routinely aspherical developed in conjunction with the understanding that long/soft gamma-ray bursts result from tightly collimated beams of gamma rays from some varieties of Type Ic supernovae (Woosley & Bloom 2006). Surely there is a close connection between the asymmetry of normal core-collapse supernovae and those that yield gamma-ray bursts. For Type Ia supernovae, the knowledge that they are asymmetric is a challenge for their ever more precise use as cosmological tools.

2. HISTORY

2.1. Predictions of Supernovae Polarization

Wolstencroft & Kemp (1972) argued that an intrinsic magnetic field dispersed by a supernova explosion might induce optical circular polarization. Shakhovskoi (1976) proposed that electron scattering in an asymmetric, expanding envelope is the most likely source of any intrinsic polarization. Shapiro & Sutherland (1982) conducted the first quantitative study of polarimetry as an important tool to study the geometry of supernovae. They found that a mixture of scattering and absorption can yield a significantly higher degree of polarization than expected from the classical, pure scattering atmosphere discussed by Chandrasekhar (1960). More sophisticated models (Höflich 1991) predicted that, for a given axis ratio, the extended atmospheres expected for supernovae would provide even more polarization than a plane-parallel atmosphere.

McCall (1984) argued that lines that form P-Cygni scattering profiles in expanding atmospheres with noncircular isophotes should show a linear polarization greater than that in the continuum. He predicted that the polarization should increase at the absorption minimum as the absorbing material blocks predominantly unpolarized forward scattered flux from the portion of the photosphere along the line of sight. This would increase the relative proportion of polarized flux that scatters from the asymmetric limb. There is also a tendency for the polarization to decrease at the emission peak because the emitted unpolarized flux tends to dilute the underlying polarized continuum flux. The result has been characterized as an inverse P-Cygni polarization profile across an unblended P-Cygni line in the flux spectrum (see P-Cygni Line Profiles sidebar).

2.2. Early Observational Attempts

Serkowski (1970) first reported supernova polarization observations. Other early attempts were made by Shakhovskoi & Efimov (1972), Wolstencroft & Kemp (1972), Lee et al. (1972), and Shakhovskoi (1976). It is not clear whether these data represent anything but interstellar polarization (ISP).

McCall et al. (1984) presented the first spectropolarimetric (SP) data on a supernova, the Type Ia SN 1983G in NGC 4753 near maximum light. They did not observe any change in polarization through the P-Cygni lines. The polarization at approximately 2% probably resulted

P-CYGNI LINE PROFILES

P-Cygni line profiles form when outflow from a source, the star P-Cygni or a supernova, yields an expanding atmosphere such that there is emission at the rest wavelength of a line from the transverse flow and blue-shifted absorption in which the flow expanding toward the observer obscures the photosphere.

from the ISP (see Section 3.3). They also looked for circular polarization, but none was detected. McCall (1985) reported observations of the Type Ib SN 1983n close to maximum light and noted that the polarization dipped from approximately 1.4% in the continuum to approximately 0.8% in the Fe II feature with no change in position angle, strongly suggesting an intrinsic polarization. Unfortunately, the data were never published. Spyromilio & Bailey (1993) obtained spectropolarimetry of the Type Ia SN 1992A both 2 weeks and 7 weeks after maximum light. They observed no significant variations across the spectral features.

The first events for which investigators obtained systematic spectropolarimetry were SN 1987A, an explosion in a rare blue supergiant, and SN 1993J, an explosion in a star nearly stripped of its hydrogen envelope. These two events (discussed in detail below) illustrate how poor the overall database of supernova spectropolarimetry was up through the early 1990s.

In 1994 we began a program to obtain spectropolarimetry of as many supernovae as possible that were visible from McDonald Observatory. At the time, only a handful of events had been examined, and there were virtually no statistics. The first few supernovae our group studied (and those in the previous sparse record such as SN 1987A and SN 1993J) were classified as peculiar in some way, so we did not know whether we were seeing incidental peculiarities or something truly significant.

As data accumulated, however, this uncertainty was removed, and significant new insights were revealed. With more data and better statistics, we identified the first key trend: The data were bimodal (Wang et al. 1996). Type Ia supernovae showed little or no polarization signal near and after maximum light (we discuss the prominent premaximum polarization below). Supernovae thought to arise by core collapse in massive stars were, by contrast, all significantly polarized. So far every core-collapse supernova for which we or other groups have obtained adequate data has been substantially polarized. Core-collapse supernovae are definitely not spherically symmetric. **Table 1** lists supernovae observed with photometric or spectroscopic polarimetry.

3. INTRODUCTION TO SUPERNOVA SPECTROPOLARIMETRY

3.1. Stokes Parameters

We can characterize the polarization of an incoming signal by its Stokes vector, S, that comprises four components, or Stokes parameters: I, Q, U, and V (Chandrasekhar 1960), where I is the intensity, Q and U measure the linear polarization, and the component V measures the circular polarization. Although a portion of the light from a supernova may be circularly polarized, low-flux levels have precluded any serious attempt to measure circular polarization, and we do not consider it here. The Stokes vector has an amplitude and a direction, but because it is related to the intensity (which is the square of the amplitude of the electric vector), it is a quasi-vector for which the directions 0° and 180° are identical.

In general, I is the total flux, and $\hat{Q}$ and $\hat{U}$ are differences in flux with the electric vector oscillating in two orthogonal directions on the sky, with $\hat{U}$ representing angles on the sky that are rotated by 45° with respect to those sampled by $\hat{Q}$. Throughout this review, we define the normalized Stokes parameters as $Q = \hat{Q}/I$ and $U = \hat{U}/I$. In this way, we express the degree of linear polarization, P, and the polarization angle, θ, in terms of the Stokes parameters as

$$P = \frac{\sqrt{\hat{Q}^2 + \hat{U}^2}}{I} = \sqrt{Q^2 + U^2} \tag{1}$$

and

$$\theta = \frac{1}{2} \arctan \frac{\hat{U}}{\hat{Q}}, \tag{2}$$

Table 1 Supernovae with polarimetric data

Supernova	Host galaxy	Type	Photometric (P) or spectroscopic (S)	No. of epochs: epoch with respect to optical maximum (SP type)	References
1968L	M83 (NGC5236)	IIP	P (undetermined)	1:	1
1970G	M101 (NGC5457)	IIL	P	1:	2
1972E	NGC 7723	Ia	P (undetermined)	3:	3
1975N	NGC 7723	Ia	P (undetermined)	2: 0, 34	4
1981B	NGC4536	Ia	P (undetermined)	1: 56	5
1983G	NGC 4753	Ia	S (undetermined)	1: −2	6
1983N	M83 (NGC 5236)	Ib	S	1: 1	6
1986G	NGC5128	Ia	S	2: −9, −8	7
1987A	LMC	IIpec	P, S	Many (D1, 2)	8
1992A	NGC 1380	Ia	S (undetermined)	1: 12 (N)	9
1993J	M81	IIb	P, S	17 (D1, L): −15, −14, −11 +2(x2), +8, +9, +10, +12 +23, +26 Plus 6 photometry	10
1994D	NGC 4526	Ia	P (undetermined)	1: −10	11
1994Y	NGC 5371	IIn	P	1: >180 (D0?)	11
1994ae	NGC 3370	Ia	P	1: >30 (N0)	11
1995D	NGC 2962	Ia	P	2: 14 (N0), 41 (N0)	11
1995H	NGC 3526	II	P	1: >33	11
1995V	NGC 1087	II	P	1?:	12
1996B	NGC 4357	IIb	S	1?:	13
1996W	NGC4027	II	S	1:	12
1996X	NGC 5061	Ia	S	1: (N1)	14
1996cb	NGC 3510	IIb	S	4: 1, 36, 40, 64 (D1, L)	15
1997X	NGC 4691	Ic	S	2: ∼5, ∼30 (D1, L)	15
1997Y	NGC 4675	Ia	S	1: (N0)	12
1997bp	NGC 4680	Ia	S	2: (D0)	12
1997bq	NGC 3147	Ia	S	1: (D1)	12
1997br	E 576-G40	Ia	S	1: (D1)	12
1997dq	NGC 3810	Ib	S	1: (D1)	16
1997ds	MCG -01-57-007	II	S	1: (D1)	17
1997dt	NGC 7448	Ia	S	1: (N1)	18
1997ef	UGC 4107	Ib/c (high velocity)	S	2?: (N1)	19
1997eg	NGC 5012	IIn	S	3: 16, 44, 93 post-discovery (D1)	20
1997ei	NGC 3963	Ic	S	1:	12
1998A	IC 2627	II	S	1:	17
1998S	NGC 3877	IIn	S	3: −14, 10, 41 (D)	21
1998T	NGC 3690	Ib	S	1:	16

(*Continued*)

Table 1 (*Continued*)

Supernova	Host galaxy	Type	Photometric (P) or spectroscopic (S)	No. of epochs: epoch with respect to optical maximum (SP type)	References
1998bw	E 184-G82	Ic (pec)	S	2: −6, 10 (N)	22
1999by	NGC 2841	Ia (subluminous)	S	3: −2, −1, 0 (D1)	23
1999em	NGC 1637	IIP	P, S	7: 7, 10, 40, 49, 73 (D), 159, 163 (post-discovery)	24
1999gi	NGC 3184	II	S	1: (D, L)	17
2001V	NGC 3987	Ia	S	1: (D1, N)	25
2001X	NGC 5921	II	S	1: (D)	25
2001bb	IC 4319	Ic	S	1: (D1)	25
2001dh	MCG -6-44-26	II	S	2: (D, L)	25
2001dm	NGC 749	Ia	S	1: (N, D)	25
2001du	NGC 1365	IIP	S	1: (N, D)	25
2001el	NGC 1448	Ia	S	5: −4 (D1, L), +2 (D1, L) +11 (D), +20 (N1), +41 (N1)	26
2001ig	NGC 7424	IIb	S	3: +13 (D, L), +31 (D, L), +256	27
2002ap	M74 NGC 628	Ic (high velocity)	S	12: −6 (N, L), −2 (N, L), 0 (D, L) +1(x2) (D, L), +2, +3(x2), +5, +26, +27, +29	28
2002bo	NGC 3190	Ia	S	2: (L)	25
2002el	NGC 6986	Ia	S	1: (D)	25
2002fk	NGC 1309	Ia	S	2: (D)	25
2002bf	CGC G266-031	Ia	S	1: (N)	18
2002ic	A013002+2153	Ia (pec)	S	5: 221 (D1), 232 (D1) 253 (D1), 255 (D1), 315 (D1)	29
2003B	NGC 1097	II	S	1: (D)	25
2003L	NGC 3506	Ic	S	1: (D)	25
2003W	UGC 5234	Ia	S	1: (D)	25
2003bu	NGC 5393	Ic	S	2: (D)	25
2003dh	A104450+213117	Ic (high velocity)	S	2: 15 (N), 16 (N)	30
2003du	UGC 9391	Ia	S	1: (D)	18
2003ed	NGC 5303	IIb	S	1:	38
2003ee	A113324-0959	IIn	S	1: (D1)	25
2003eh	M+01-29-03	Ia	S	1: (N1)	25
2003gd	M74 NGC 628	IIP	S	1: (D)	25
2003gf	MCG -04-52-026	Ic	S	1:	38
2003hh	UGC 12890	Ia	S	2: (D1)	25
2003hv	NGC 1201	Ia	S	1: (D)	25
2003hx	NGC 2076	Ia	S	1: (D)	25
2003hy	IC 5145	IIn	S	1: (D1)	25
2004S	MCG -05-16-021	Ia	S	1: (D)	31

(*Continued*)

Table 1 (*Continued*)

Supernova	Host galaxy	Type	Photometric (P) or spectroscopic (S)	No. of epochs: epoch with respect to optical maximum (SP type)	References
2004dj	NGC 2403	II	S	1: (D)	32
2004dk	NGC 6118	Ib	S	1: (D)	25
2004dt	NGC 799	Ia	S	2: −7 (D1, L), +4 (D1, L)	33
2004br	NGC 4493	Ia (pec)	S	1: (N1)	25
2004dk	NGC 6118	Ib	S	1: (D1)	25
2004ef	UGC 12158	Ia	S	1: (D1)	25
2004eo	NGC 6928	Ia	S	1: (D1)	25
2005bf	MCG+00-27-005	Ib/c	S	1: −6 (wrt second max) (D1, L)	34
2005cf	MCG –1-39-3	Ia	S	1: (N1)	25
2005de	UGC 11097	Ia	S	2: (N1)	25
2005df	NGC 1559	Ia	S	2: (D1)	25
2005el	NGC 1819	Ia	S	1: (D1)	25
2005hk	UGC 272	Ia (pec)	S	3: −4 (D1), 0 (D1), +14 (D1)	35
2005ke	NGC 1371	Ia	S	2: (D1)	25
2006X	NGC 4321	Ia	S	9: −10 (D1, L), −8 (D1, L) −7 (D1, L), −6 (D1, L), −3 (D1, L) −2 (D1, L), −1 (D1, L), +39 (N1)	36
2006aj	A032140+165203	Ib/c (XRF)	P, S	9: −7 (N1), −6 (N1), −5 (N1) −4 (N1), 0 (N1), +3 (N1) +8 (N1), +29 (N1), 300? (N0)	37
2006bc	NGC 2397	II	S	1: (D)	25
2006be	IC 4582	II	S	1: (D)	25
2007af	NGC 5584	Ia	S	2:	25
2007fb	UGC 12859	Ia	S	4:	25
2007hj	NGC 7461	Ia	S	3:	25
2007if	Anon	Ia	S	5:	25
2007it	UGC 10553	II	S	3:	25
2007le	NGC 7721	Ia	S	3:	25
2008D	NGC 27720	Ib/c (pec)	S	2: (D1)	25

References: (1) Serkowski 1970, Wood & Andrews 1974; (2) Shakhovskoi & Efimov 1972; (3) Lee et al. 1972, Shakhovskoi 1976, Wolstoncroft & Kemp 1972; (4) Shakhovskoi 1976; (5) Shapiro & Sutherland 1982; (6) McCall et al. 1984, McCall 1985; (7) Hough et al. 1987; (8) Cropper et al. 1988, Méndez et al. 1988; (9) Spyromilio & Bailey 1993; (10) Trammell, Hines & Wheeler 1993; Doroshenko, Efimov & Shakhovskoi 1995, Tran et al. 1997; (11) Wang et al. 1996; (12) Wheeler 2000; (13) mentioned in Wang et al. 2001; (14) Wang, Wheeler & Höflich 1997; (15) Wang et al. 2001; (16) Leonard, Filippenko & Matheson 2000; (17) Leonard & Filippenko 2001; (18) Leonard et al. 2005; (19) Leonard et al. 2000, Wheeler 2000; (20) Leonard et al. 2000; (21) Leonard et al. 2000, Wang et al. 2001; (22) Patat et al. 2001; (23) Howell et al. 2001; (24) Leonard et al. 2001, Wang et al. 2001; (25) D. Baade, J.R. Maund, P. Höflich, F. Patat, L. Wang, J.C. Wheeler, unpublished; (26) Wang et al. 2003a; (27) Maund et al. 2007c; (28) Kawabata et al. 2002, Leonard et al. 2002a, Wang et al. 2003b; (29) Wang et al. 2004, K. Kawabata, unpublished; (30) Kawabata et al. 2003; (31) Chornock & Filippenko 2006; (32) Leonard et al. 2006; (33) Leonard et al. 2005, Wang et al. 2006; (34) Maund et al. 2007b; (35) Chornock et al. 2006, J.R. Maund, J.C. Wheeler, F. Patat, L. Wang, D. Baade, P. Höflich, in preparation; (36) F. Patat, D. Baade, P. Höflich, J.R. Maund, L. Wang, J.C. Wheeler, in preparation; (37) Gorosabel et al. 2006, Mazzali et al. (2007), Maund et al. 2007a; (38) Leonard & Filippenko 2005.

or

$$Q = P \cos 2\theta, \quad U = P \sin 2\theta. \tag{3}$$

The astronomical convention is that $\theta = 0°$ points to the north on the sky.

3.2. Observational Techniques

Many researchers have presented the basic techniques of spectropolarimetry (Miller & Goodrich 1990, Goodrich 1991, del Toro Iniesta 2003, Patat & Romaniello 2006; see also van de Hulst 1957). Because polarimetry involves the difference of the ordinary and extraordinary light rays that have passed through the polarization analyzer, usually a Wollaston prism (del Toro Iniesta 2003), the per-pixel errors are exaggerated compared with those in the total flux spectra and are artificial because each resolution element contains more than one pixel. It is therefore useful to rebin the data into bin sizes comparable to the spectral resolution to reduce the artificial per-pixel errors and error correlations. One must also be careful that estimates of polarization from Equation 1 are not biased to large values by noise (Simmons & Stewart 1985; Wang, Wheeler & Höflich 1997). [For a detailed discussion of procedures involved in reducing supernova spectropolarimetry data, see Wang, Wheeler & Höflich (1997), Leonard et al. (2001, appendix 1), Leonard & Filippenko (2001), Leonard et al. (2002a, appendix), Wang et al. (2003a), Patat & Romaniello (2006), Maund et al. (2007a), Maund (2008).]

3.3. Interstellar Polarization

Polarization introduced by interstellar dust in either the host galaxy or the Milky Way Galaxy can complicate the interpretation of observed polarization. Fortunately, the wavelength dependence of the ISP is well quantified by observations of Galactic stars (Serkowski et al. 1975, Whittet et al. 1992). The polarization from supernova ejecta is expected to vary across spectral lines, and the wavelength dependence may be different. The supernova polarization also varies in time, whereas the ISP does not. In principle, these features allow the separation of the supernova polarization from the contributions of the ISP.

There is no completely satisfactory method to derive the ISP of supernova polarimetry observationally. Many methods have been proposed, but they have to make assumptions about the supernova polarization, including that certain components of the supernova spectrum, such as the emission peaks of P-Cygni profiles, are not polarized (Trammell, Hines & Wheeler 1993; Tran et al. 1997) and that the blue end of the supernova spectra is unpolarized because of strong line-blended depolarizing lines (Wang et al. 2001). Some methods implicitly assume a simple axially symmetric geometry of the ejecta, which is often ruled out by the observational data. It is thus often dangerous to derive scientific results assuming that one has accurate a priori knowledge of the ISP.

If the ISP is significantly larger than the intrinsic polarization of a supernova, the wavelength dependence of the observed polarization can provide estimates of the properties of the dust particles along the line of sight to the supernova. We can compare an estimate of the wavelength at which the ISP reaches its maximum with that for the Galaxy, at approximately 5500 Å, to see if the mean properties of the host dust are similar or different. Hough et al. (1987) probed the ISP due to the dust lanes in Centaurus A by observing SN 1986G, and they concluded that the size of dust particles is smaller than typical Galactic dust particles. Recently Wang et al. (2003a) studied the dust properties in NGC 1448 and found their size to be slightly smaller than their Galactic counterparts. Leonard et al. (2002b) observed a highly reddened Type II plateau supernova (see Section 4.3.1), SN 1999gi in NGC 3184, and found that the polarization efficiency of the dust in

NGC 3184 was much higher than typical Galactic dust. It is important to get more polarization data of highly extincted supernovae as this is a powerful tool to study the elusive properties of extragalactic dust.

3.4. The Dominant Axis

The prominent spectral features of supernovae make it possible to deduce valuable information without accurate estimates of the ISP. Wang et al. (2003a) outlined a method to decompose the observed polarimetry into two components, equivalent to a two-component principal component analysis. In the *Q/U* plane, the two components correspond to the polarized vectors projected onto the so-called dominant axis and onto the axis perpendicular to the dominant axis, which we refer to as the orthogonal axis. A dominant axis can often be defined from the distribution of the data points on the *Q/U* plane (Wang et al. 2001). The spectropolarimetry projected onto the dominant axis represents global geometric deviations from spherical symmetry, whereas the vector perpendicular to the dominant axis represents physical deviations from the dominant axis. One can determine the coordinates of the new system by rotating the original coordinates counterclockwise so that the *Q* axis overlaps the dominant axis in the new coordinate system, and the dominant axis points toward the center of the data cluster on the *Q/U* plane. The components parallel and perpendicular to the dominant axis are given by

$$P_d = (Q - Q_{ISP})\cos\alpha + (U - U_{ISP})\sin\alpha \quad (4)$$

and

$$P_o = -(Q - Q_{ISP})\sin\alpha + (U - U_{ISP})\cos\alpha, \quad (5)$$

where P_d and P_o are the polarization components parallel to the dominant axis and orthogonal to that axis, respectively; Q_{ISP} and U_{ISP} are the Stokes parameters of the ISP; $\alpha = 2\theta_d$ is the rotation angle in the *Q/U* plane; and θ_d is the polarization position angle of the dominant axis. One advantage of using these decomposition formulae rather than calculating the degree of polarization as given by Equations 1 and 2 is that the spectral profiles of P_o and P_d are insensitive to the choice of ISP. Leonard et al. (2001) employed a similar procedure producing rotated Stokes parameters by calculating a fit to the continuum position angle so that all the continuum polarization falls on the rotated Q. This is equivalent to, but not quite the same technically, as fitting a dominant axis in the *Q/U* plane. The polarization spectral profiles of the decomposition method may not depend on the unknown ISP.

If the supernova ejecta are smooth and axially symmetric, the data points on the *Q/U* diagram should follow a straight line defining the dominant axis, as expected from theoretical models (Höflich et al. 1996). If the geometry departs significantly from axial symmetry, the data points show noticeable dispersion from a straight line, in the direction of the orthogonal axis. **Figure 1** illustrates these basic situations and their representation in the *Q/U* plane schematically.

For homologous expansion, $v \propto r$, surfaces of constant velocity are planes normal to the line of sight. Viewing at different wavelengths through a line profile corresponds to viewing the geometry along different slices normal to the line of sight. In general, owing to the interplay of geometry and optical depth, different wavelengths register different amplitudes of polarization and hence values of *Q* and *U*. For an axisymmetric structure the observations will all be at a fixed angle, and simple rotation of the coordinates aligns the rotated *Q* axis with the line representing the dominant axis (**Figure 1**, top). In this simple example, there is no contribution along the orthogonal axis corresponding to the rotated *U* axis. The distribution along the orthogonal axis will reveal any clumpy, nonaxisymmetric structure (**Figure 1**, bottom).

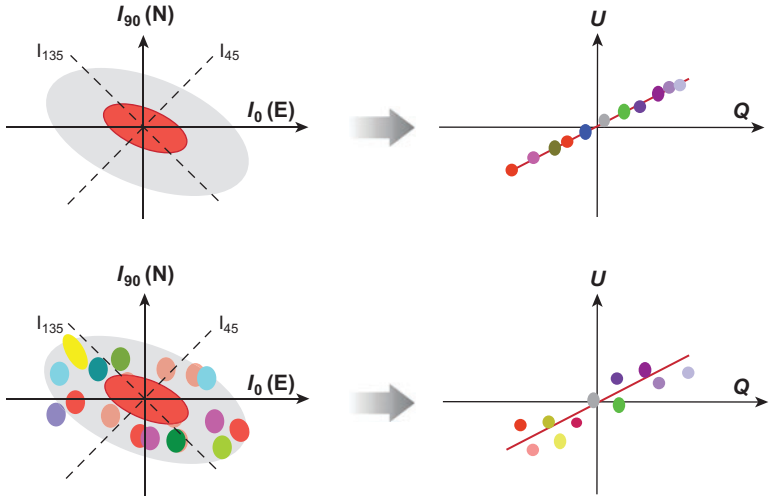

Figure 1

(*Top left panel*) A smooth, axisymmetric structure with the axis tilted at an arbitrary position angle on the sky and with respect to the line of sight. The directions denoted by *I* represent the measurement of the flux at the angles needed to construct the *Q* and *U* polarization components. (*Top right panel*) The resulting wavelength-dependent polarization amplitude plotted in the *Q/U* plane follows a straight line, the dominant axis. The colored circles represent the polarization measured at different wavelengths. (*Lower left panel*) A case for which the axisymmetry is broken into clumps of different composition and optical depth. Clumps of high-opacity absorbing material block parts of the underlying photosphere, which induces wavelength-dependent geometry even if the underlying photosphere is symmetric and hence does not impose any net polarization. Clumps blocking an asymmetric photosphere yield more complex structure, but no difference in principle. (*Lower right panel*) The polarization distribution in the *Q/U* plane in general is no longer along a straight line. The basic axisymmetric geometry may still be evident, but the departure from axial symmetry caused by the clumping yields a finite, and physically significant, distribution along the orthogonal axis. The *Q/U* diagrams in the upper and lower right panels represent spectropolarimetry Types D0 and D1, respectively.

The decomposition of the polarization components given by Equations 4 and 5 assumes the existence of only two components with fixed axes: an ISP component and one additional component that is intrinsic to the supernova. This is clearly an oversimplification for some events that need a more complicated decomposition. A more realistic approach is to assume that the line polarization and continuum polarization have independent geometries and that the observed polarization is a combination of the two.

Although there are numerous ways to present and analyze spectropolarimetry data, displaying the data in the *Q/U* plane facilitates doing the requisite vector analysis by eye. One can immediately and directly see how the amplitude and polarization angle change by modifying the placement of the always uncertain and frequently controversial ISP. Likewise, the tendency of the data to fall along a single axis, or to depart from a primary axis in loops or other structures, is transparent, completely independent of the placement of the ISP. We take advantage of this power in the subsequent analysis.

3.5. Loops in the *Q/U* Plane

In general, the continuum polarization from a supernova provides information about the overall shape of the photosphere, whereas the polarization across spectral lines is more sensitive to

small-scale structures in the ejecta. Large-scale gradients in density and composition structure may also affect line polarization, but such effects are generally saturated for strong lines owing to their large optical depth.

If the composition structure is complex, then the degree and angle of polarization may vary significantly across strong spectral lines, which produces loops in the *Q/U* plane. These loops are loci on the *Q/U* plane that are functions of the wavelength across the line feature and hence functions of the velocity and of the depth of the portion of the structure that contributes to that wavelength. Because the loops represent changes in the amplitude and angle of polarization as a function of wavelength, velocity, and depth, they specifically provide evidence for the breakdown of axial symmetry. The loops could be caused by composition-dependent clumps or more organized structures that nevertheless break the axial symmetry.

Figure 2 presents an example of how loops may be formed. It was constructed in the context of the high-velocity calcium feature of Type Ia supernovae (see Section 5.1.1), but the principles are quite general. Possible structures leading to loops, many of which are discussed by Kasen et al. (2003), include an asymmetric photosphere, different geometries for a surrounding shell, and break up of the structure into clumps. [Kasen et al. (2003) also provide an excellent pedagogical exposition of polarization in supernova atmospheres.]

As discussed below, loops in the *Q/U* plane (with their implied nonaxisymmetric structure) are common in both core-collapse and thermonuclear supernovae. These loops represent an important new clue to the physics and the structure of both types of explosion.

3.6. Spectropolarimetry Types

We can classify the spectropolarization characteristics of a supernova according to its distribution in the *Q/U* diagram. This classification scheme follows directly from the principles outlined in **Figures 1** and **2** and is insensitive to the exact value of the ISP. We define the following SP types: (*a*) SP Type N0 is characterized by polarization data with no significant deviation from a distribution that is consistent with observational noise. The centroid of the distribution may be offset from zero polarization owing to interstellar dust, but there is no measurable supernova polarization. There is no dominant axis. (*b*) SP Type N1 is characterized by polarization data with no significant elongation in any preferred direction, but for which the data distribution is wider than would be consistent with the observational errors, indicating intrinsic polarization or systematic underestimate of observational error. There is no dominant axis. (*c*) SP Type D0 is characterized by data that show an elongated ellipse in a *Q/U* diagram, with the distribution orthogonal to the major axis of the ellipse consistent with observational noise. The locus of the data can be well approximated by fitting a straight line (except in the case of very strong ISP and very broad wavelength coverage). The position angle of this fitted line defines the dominant axis of the data. (*d*) SP Type D1 is characterized by data that show an elongated ellipse in a *Q/U* diagram so that a dominant axis can be identified, but for which a straight line does not provide a satisfactory fit. Significant deviations are found orthogonal to the dominant axis. (*e*) SP Type L is characterized by some supernovae that show large significant changes in the amplitude and position angle across strong spectral lines. These variations result in prominent loops on the *Q/U* diagram.

In general, one deduces the SP type from observations at a certain epoch and in a certain wavelength range. The SP properties of supernovae evolve with time, so the SP type as defined here can evolve as well. In addition, different portions of the spectrum may reveal different characteristics. The continuum or a single line could be a type D0, whereas another line could be a type L. We

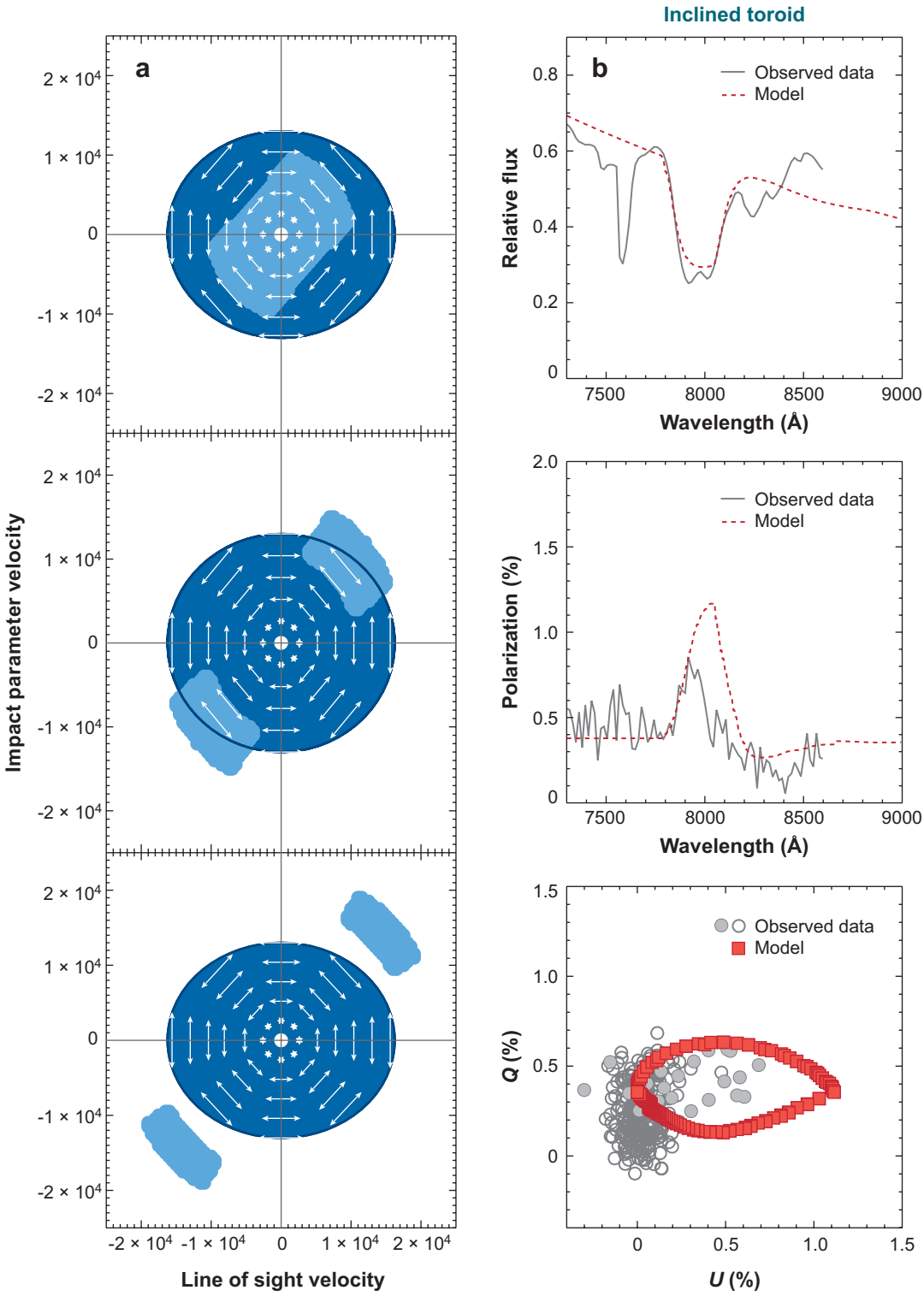

have assigned tentative SP types to those supernovae in **Table 1** in cases justified by the data. We also use this classification to discuss individual events below.

To characterize the data, one must correctly estimate both the systematic and the statistical observational errors. In additional to normal SP calibrations such as from observations of polarized and unpolarized standard stars, it is highly advisable to acquire two complete sets of polarization data each night. This allows one to cross-check the errors and stability of the spectropolarimetry with data taken with identical observational setups.

4. CORE-COLLAPSE SUPERNOVAE

4.1. General Trends: Evidence for Bipolar Explosions in the Machine

The most important conclusion from the study of supernova spectropolarimetry is that the process of core collapse routinely involves an intrinsically, strongly aspherical explosion mechanism that is directed substantially along a single direction in space. Prior to these spectropolarimetric studies, the explosion was assumed to be substantially spherical, with any departures from spherical symmetry resulting from rather small-scale effects of convection or Rayleigh-Taylor instabilities. The evidence for strongly directed explosions has given rise to a new literature of jet-induced explosions and variations on that theme (Khokhlov et al. 1999; MacFadyen & Woosley 1999; Wheeler et al. 2000; Wheeler, Meier & Wilson 2002; Maeda & Nomoto 2003; Shibata et al. 2003; Kotake et al. 2004; Yamada & Sawai 2004; Burrows et al. 2006, 2007; Kifonidis et al. 2006; Obergaulinger et al. 2006; Komissarov & Barkov 2007, and references therein; Blondin & Mezzacappa 2007; Moiseenko & Bisnovatyi-Kogan 2007). It has also established a strong tie to cosmic, long gamma-ray bursts that also involve the collapse of massive stars and highly directed energy output (Woosley & Bloom 2006). Major efforts are now underway to understand the origin of the asymmetry, most plausibly in terms of rotation and magnetic field in the progenitor and newly formed neutron star (Akiyama et al. 2003; Thompson, Chang & Quataert 2004; Masada, Sano & Takabe 2006; Uzdensky & MacFadyen 2007, and references therein). The spectropolarimetry of core-collapse supernovae has thus helped catalyze a paradigm shift in the thinking about the explosion mechanism.

We now recognize that a dominant axis in the polarimetry represents a primarily axisymmetric activity. Below we summarize in some detail how the data that led to this conclusion were attained, revisit SN 1987A and SN 1993J in the current context, and attempt to establish a common framework for the interpretation of the data. We establish that polarization is not a feature of a few odd core-collapse supernovae, but a generic feature of every spectral type. A recent key conclusion is that, although a bipolar structure is dominant in the geometry of core-collapse supernovae, departures from axisymmetry evidenced by loops in the *Q/U* plane and other composition-dependent structures are also ubiquitous and must be incorporated in physical models.

←

Figure 2

(*a*) Velocity slices through an edge-on torus surrounding an ellipsoidal photosphere, both expanding homologously. This geometry breaks the axisymmetry. The torus has a strong absorption line that blocks the continuum emission from the photosphere. The geometry of the blocking region depends on the velocity slices through the structure and hence on the wavelength across the line profile. The arrows mark the photospheric polarization angle and amplitude. The three panels (*from top to bottom*) show decreasing blue shift. (*b*) The effect of the torus, now tilted both with respect to the line of sight and to the axis of the underlying ellipsoidal photosphere, on the total flux line feature, the polarization feature, and as depicted in the *Q/U* plane. The polarization is somewhat strong compared to the particular observations of the Type Ia supernova SN 2001el (*gray*), but the locus in the *Q/U* plane shows a loop that matches the observations rather well (*red*). Figure taken from Kasen et al. (2003).

4.2. SN 1987A

SN 1987A was the first supernova for which systematic, high-quality photometric polarimetry and SP data were obtained. Although formally a hydrogen-rich Type II supernova, the blue supergiant progenitor and detailed observations of all kinds (Arnett et al. 1989, McCray 1993) place this supernova into its own category. The polarimetric data on SN 1987A have not been adequately explored. We can view them now in the context of the larger sample of more distant supernovae. More thorough quantitative analysis clearly is warranted, but the basic themes of core-collapse supernovae are reflected here. SN 1987A displayed significant large-scale asymmetry with well-defined principal axes consistent with jet-like flow, but was also marked by departures from axisymmetry. [For a complete set of references, see Jeffery (1991b) and Wang et al. (2002a).]

4.2.1. Photometric polarimetry. Some early estimates of ISP now appear to have been incorrect and led to incorrect conclusions. With the later and probably more reliable estimate of the ISP, Jeffery (1991b) found that the polarization was small at early times and then grew monotonically for the first month (**Figure 3**). SN 1987A thus hinted at strong asymmetry of the inner machine of the explosion, evidence that has proven ubiquitous for core collapse with current, systematic observations. Theoretical models to account for the early behavior of SN 1987A were presented by Méndez et al. (1988), Jeffery (1989, 1990, 1991a), and Höflich (1991). Models based on Méndez et al.'s (1988) estimate of the ISP, which implied an early declining value of the polarization, need to be reconsidered.

Figure 3 suggests that around day 140, as the major light-curve maximum gave way to the exponential radioactive tail, the polarization jumped to 1.3%–1.5% and then slowly dropped back to approximately 0.2%–0.4% by day 200. This jump might be associated with the photosphere receding through the outer hydrogen envelope and revealing the inner core. Whether the polarization of SN 1987A was quite variable in this epoch or some of the data are questionable has not been resolved, calling for more study and careful modeling.

A remarkable fact is that the broadband polarization angle did not waver through this whole evolution, including the possible large spike in the broadband polarization. The second speckle source, the mystery spot (see Mystery Spot in SN 1987A sidebar), and the orientation of the late-time Hubble Space Telescope image of the ejecta at $\theta \sim 16°$ provide another measure of the orientation (Wang et al. 2002a). For brevity, we refer to this as the speckle angle below. Scattering from features aligned in this direction gives a plane of polarization with a position angle of 106°. Within observational uncertainty, this is close to the position angle of the continuum polarization. The position angle of the minor axes of the circumstellar rings is also aligned close to the position angle determined from the dominant axis of polarization.

By these measures, we can see that SN 1987A pointed in a certain direction, a position angle of $\theta \sim 16°$, and maintained that orientation throughout its development (Wang et al. 2002a). This requires a large-scale, systematic, directed asymmetry that cannot be accounted for by

MYSTERY SPOT IN SN 1987A

The mystery spot associated with SN 1987A (Dotani et al. 1987, Meikle et al. 1987, Nisenson & Papaliolios 1999) was a small source of luminosity detected in speckle imaging that was nearly as bright as the supernova. No thoroughly satisfactory explanation has been provided.

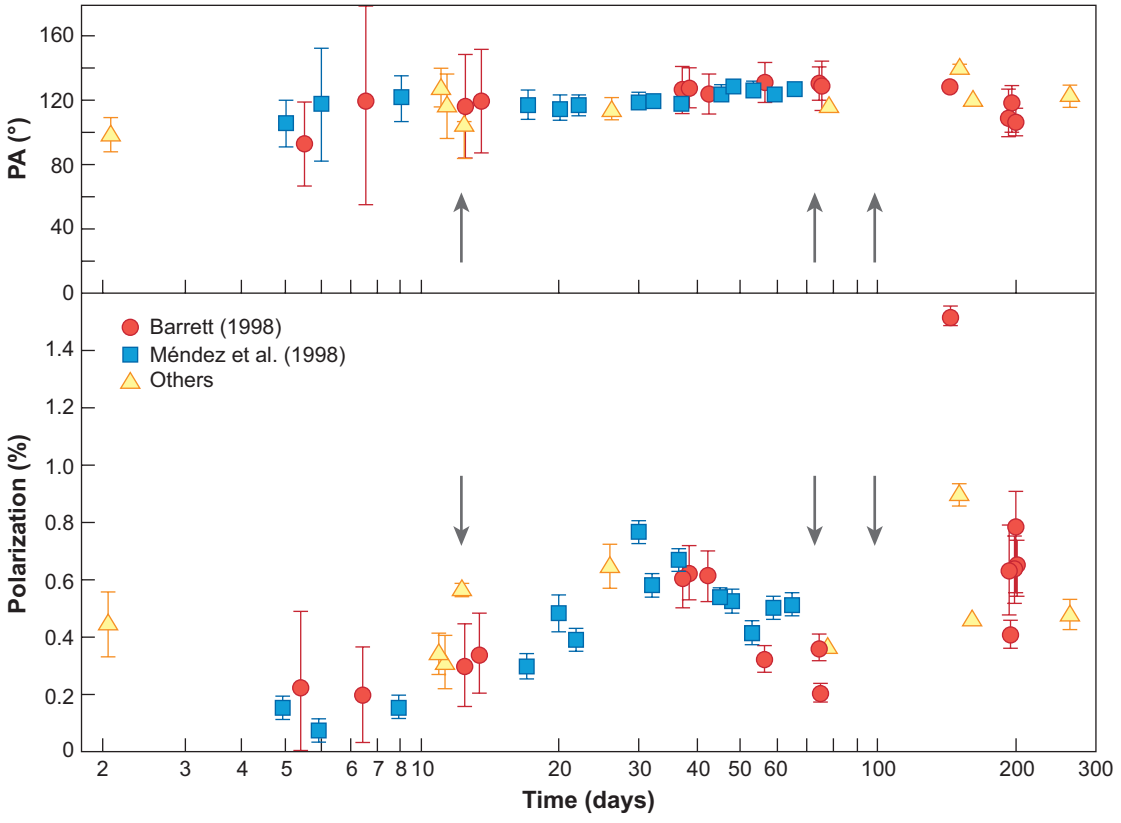

Figure 3

Evolution of the V-band polarization and associated polarization angle (PA) of SN 1987A. Note the near constancy of the polarization angle despite the variation in the amplitude of the broadband polarization. Vertical arrows indicate the epochs for which spectropolarimetry is presented in **Figures 4** and **5**. Data taken from Jeffery (1991b).

small-scale convection or turbulence. The continuum polarization probes the geometric structure of the photosphere. The persistent polarization position angle of the dominant axis across a broad wavelength range and the lack of significant evolution of the polarization position angle strongly argue for a shared geometry for the early and late epoch photospheres. The data also show that the overall structure of SN 1987A was remarkably axially symmetric from deep inside the oxygen-rich zone, out to the hydrogen envelope, and on to the circumstellar rings. The totality of the data suggests that the angular momentum of the progenitor system played a crucial role in the explosion of SN 1987A (Wang et al. 2002a). Although most of the polarization of SN 1987A is intrinsic, some effects may be induced by dust scattering in the asymmetric environment (Wang & Wheeler 1996).

4.2.2. Spectropolarimetry. The first spectropolarimetry of SN 1987A, obtained on March 8, 1987, was presented by Schwarz & Mundt (1987) and was modeled by Jeffery (1987). Clocchiatti & Marraco (1988) also reported broadband polarimetry. Cropper et al.'s (1988) subsequent excellent spectropolarimetry confirmed that, as data are tracked as a function of wavelength over spectral features, the polarization angle does sometimes change with wavelength, giving rise to loops in the *Q/U* plane. As explained in Section 3.5, as wavelength varies over a Doppler-broadened line

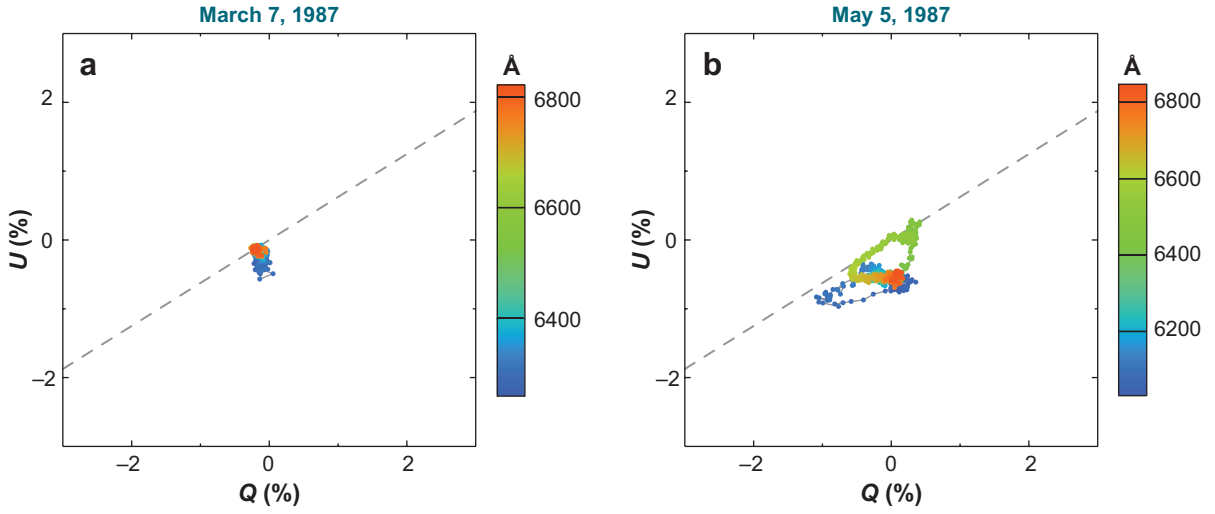

Figure 4

(*a*) Hα and adjacent continuum in the *Q/U* plane for SN 1987A on March 7, 1987, approximately 2 weeks after the explosion. The data cluster near the origin with some small departure to negative U at a position angle of approximately 150°. (*b*) Hα and adjacent continuum on May 5, 1987, near maximum light. The Hα polarization developed a distinct loop structure, indicating significant departures from axisymmetry with little relation to the data from March 7. The dashed line corresponds to the speckle angle ($\theta \sim 16°$) (Meikle et al. 1987) in the negative quadrant, extrapolated into the positive quadrant as if there were an oblate counterpart to guide the eye. The data have been corrected for the interstellar polarization given by M. Méndez (private communication) and Jeffery (1991b). Figure adapted from Cropper et al. (1988).

feature, different depths are sampled in the ejecta, with a given wavelength sampling a velocity slice through the ejecta normal to the line of sight. The presence of loops implies that the polarization amplitude and angle vary along those velocity/depth slices. This variation means that there must be some substantial departure from axisymmetry in SN 1987A imposed on the overall pointed behavior revealed by the photometric polarimetry. This SP behavior gives a rich phenomenology that is ripe for progress in the physical understanding of SN 1987A. These loops give greater insight into the composition-dependent, three-dimensional structure of the ejecta and are worth studying in more depth than allowed here. Below we demonstrate that these loops and the implied nonaxisymmetry are not unique to SN 1987A, but are instead common to all core-collapse events.

We describe here some of Cropper et al.'s (1988) data corrected for the ISP using M. Méndez's (private communication) data as parameterized by Jeffery (1991b). When the supernova was approximately 12 days old, the data in the vicinity of the Hα line extended to negative U values, corresponding to a position angle $\theta \sim 150°$ with respect to the polarized continuum adjacent to the line (**Figure 4*a***). This is similar to, but perhaps significantly different than, the nearly time-independent V-band position angle $\theta \sim 120°$ in **Figure 3** and the speckle angle.

Figure 4*b* shows the dramatically different distribution of the Hα polarization in the *Q/U* plane when the supernova was approximately 70 days old and approaching maximum brightness. Although the inner, asymmetric core of the star has not been exposed, the variation of polarization across the Hα line has changed dramatically. The variation of *Q* and *U* with wavelength across the Hα line profile now traces out a distinct loop in the *Q/U* plane. For reference, the Hα absorption minimum at 6460 Å corresponds to the maximum positive *Q* and *U*. The distribution at this epoch has little relation to the orientation displayed at the earlier epoch in **Figure 4*a***. One significant new feature is the distinct loop structure that falls close to the speckle angle.

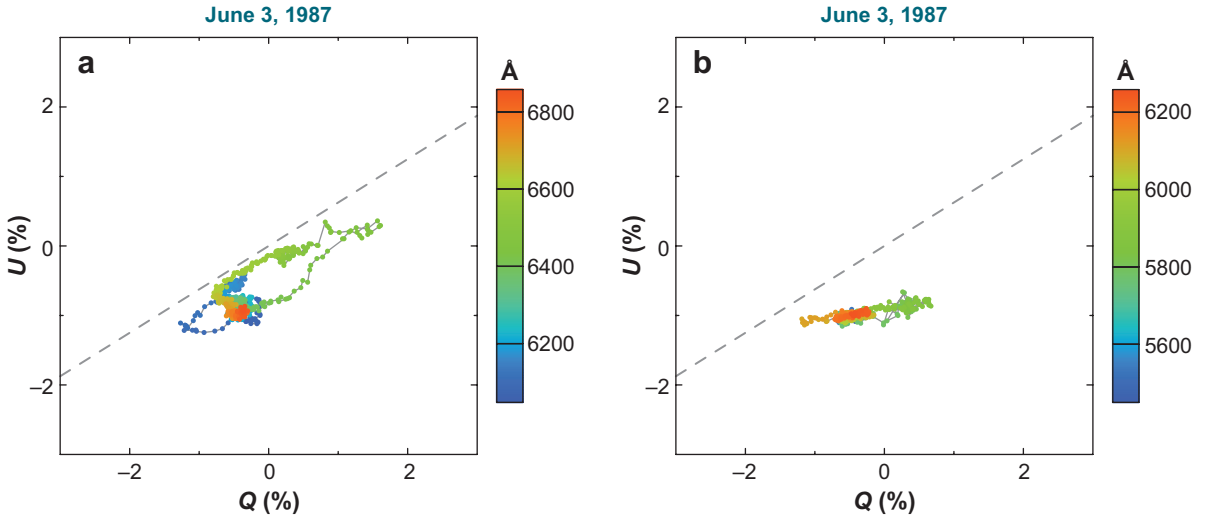

Figure 5

(*a*) Hα and adjacent continuum on the *Q/U* plane for SN 1987A on June 3, 1987, at the beginning of the fading from peak. The loop structure is now especially prominent. (*b*) He I λ5876 and adjacent continuum on June 3, 1987. The data at approximately 5600 Å and 6200 Å represent the continuum. The He I line shows a large excursion to $Q \sim 0.7\%$ at 5800 Å at absorption minimum. The data at $Q \sim -1.2\%$ at 6100 Å correspond to the absorption minimum of the adjacent Ba II line. All these features fall closely along the same locus. The dashed line corresponds to the speckle angle ($\theta \sim 16°$) (Meikle et al. 1987) in the negative quadrant and extrapolated into the positive quadrant as if there were an oblate counterpart to guide the eye. The data have been corrected for the interstellar polarization given by M. Méndez (private communication) and Jeffery (1991b). Figure adapted from Cropper et al. (1988).

Although the photosphere is still in the hydrogen envelope, the hydrogen clearly, in part, reflects the dominant asymmetry of the inner regions. A likely cause for this asymmetry is the nonspherical distribution of the ionization source in the form of a lump of radioactive nickel and cobalt (Chugai 1992). Departures from the dominant axis lead to loops associated with Hα. All the complexities displayed here are topics for more in-depth study.

The next epoch presented by Cropper et al. (1988) is on June 3, 1987, approximately 100 days after the explosion, midway through the decline of the light curve to the radioactive tail and about the time of the jump of the V-band polarization. **Figure 5** shows a sample of these data. In the vicinity of Hα, there is again a distinct extension roughly along the speckle angle, but also an interesting loop structure that reflects the nonaxisymmetric interplay of the line opacity with the polarized continuum. The absorption minimum at ~6400 Å corresponds to the data of the most extreme positive *Q* and *U*. Significant polarization, primarily along the speckle angle, is shown by Hα up to 1 year after the explosion (Cropper et al. 1988).

The He I λ5876 line and surrounding continuum illustrated in **Figure 5*b*** show remarkable uniformity. The data span $Q = 0$ at $U \sim -1$ with an exceedingly well-defined dominant axis with position angle $\theta \sim 4°$. The displacement to negative *U* results from the addition of the underlying continuum that adds a wavelength-independent component to the line polarization (Wang et al. 2003b). The polarization angle of this helium feature is not the speckle angle. The simple single-axis behavior of the helium line is in stark contrast with that of the Hα feature. Curiously, the distinct orientation of the He I line is not imprinted in any obvious way on the hydrogen geometry.

As in so many other ways, SN 1987A was also a canonical event in terms of its polarimetry. The data deserve a more thorough quantitative study than has been done, or than we can attempt

here, but several key themes emerge. The explosion was asymmetric. There is evidence from spectropolarimetry in the continuum and across the Hα line for a well-defined physical orientation that corresponds to other evidence for a substantially axially symmetric structure and jet-like flow. Conversely, there are fascinating and substantial departures from a simple bipolar explosion.

With regard to the SP types defined in Section 3.6, we can classify the data as SP Type L with respect to strong P-Cygni lines: Hα, O I, and Ca II. Across the entire optical wavelength range, the supernova shows an apparent dominant axis that is nearly constant with time and can be classified as SP Type D1. The He I line in **Figure 5** can be classified as SP Type D0.

4.3. Type II Supernovae

SN 1987A was clearly asymmetric with strong evidence for a bipolar, jet-like flow. This supernova also had obvious peculiarities; its progenitor was a blue supergiant, and a binary companion might have been involved. The question remained whether the asymmetries revealed in SN 1987A applied to general processes in core collapse. One means to address this question is to examine other Type II supernovae.

4.3.1. Type II plateau. Type IIP supernovae explode in red supergiants with extended hydrogen envelopes. Their light curves display a long phase of weeks to months of nearly constant luminosity, called the plateau phase, as the envelope expands and the photosphere recedes by recombination through the envelope. These supernovae are thought to arise in single stars of modest mass, ~10–20 $M_{\odot}$, and hence to be the most straightforward, generic type of core-collapse supernova. For that reason, it is especially important to investigate their polarization properties. Spectropolarimetry of Type IIP was reported by Leonard & Filippenko (2001) and Leonard et al. (2002b). Other examples are explored in some detail below.

For Type IIP supernovae, the polarization is usually modest on the plateau phase, but probably not zero. The density structure of the envelope is expected to be nearly spherically symmetric because conservation of angular momentum is likely to lead to slow rotation as the envelope expands after core hydrogen depletion. A likely cause of the early polarization is an asymmetric distribution of radioactive elements that distorts the ionization and excitation structure even though the density structure remains essentially spherically symmetric (Chugai 1992; Höflich, Khokhlov & Wang 2001; Khokhlov & Höflich 2001).

One of the best-studied examples of a Type II supernova is SN 1999em, which displayed a classic, if long-lived, plateau, suggesting an especially massive outer hydrogen envelope (Leonard et al. 2001, Wang et al. 2002b). Observations were obtained from approximately 1 week after discovery to approximately 6 months later. **Figure 6** shows data for SN 1999em on a *Q/U* plot. The striking feature is that the data points concentrate on a single line as the wavelength and time vary. Leonard et al. (2001, their figure 8) illustrate the same behavior, showing that the polarization of SN 1999em jumped from approximately 0.2% in the early phases to approximately 0.5% 160 days later, but with virtually no change in the polarization angle. The constancy of the position angle suggests a well-defined symmetry axis throughout the ejecta, independent of wavelength. Leonard et al. (2001, their figure 16) hint at nonaxisymmetry, but the data are insufficient for detailed study. SN 1999em was a rather typical Type II plateau explosion, yet it demonstrated the key behavior of core-collapse supernovae emphasized in this review: Its explosion was aspherical and aligned along a fixed direction in space. SN 1999em would be classified as a SP Type D0 or D1; a careful study has not been made of the dispersion in the orthogonal direction.

As a Type II plateau supernova continues to expand, the photosphere finally recedes through the hydrogen envelope, exposing the ejecta from the heavy-element core. This is accompanied

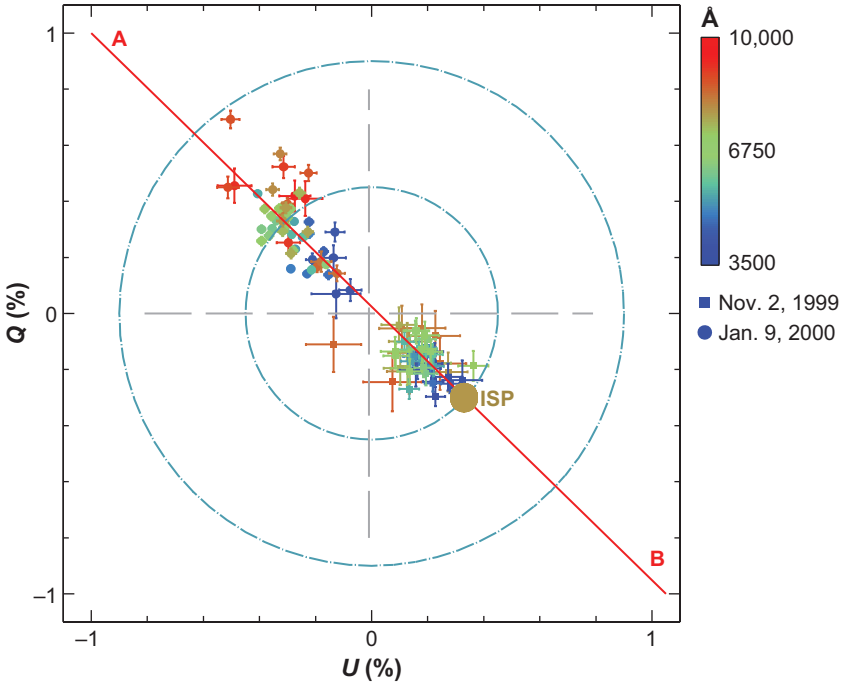

Figure 6

Polarimetry of the Type II SN 1999em. The wavelengths represented by different data points are color encoded. The November 2, 1999, data corresponding to the early plateau are clearly separated from the January 9, 2000, data on the late plateau, showing an increase in polarization with time. Line AB is the dominant axis. The circles represent the upper limits to the interstellar polarization (ISP) (measured with respect to the observed values $Q = 0$, $U = 0$) assuming that E(B-V) toward the supernova is 0.05 (*inner circle*) and 0.1 (*outer circle*). The approximate location of the component due to interstellar dust is shown as a solid circle. From Wang et al. (2002b).

by a sharp drop in luminosity, characterizing the end of the plateau phase of the light curve. The plateau phase is typically followed by an exponential decline in luminosity, consistent with the decreasing deposition of energy from radioactive decay. The polarization tends to rise rapidly at the end of the plateau phase as the photosphere enters the core ejecta. This was suggested in SN 1987A, in which the polarization jumped from 0.2% to 1.2% at 110 days as the maximum peak gave way to the radioactive decay tail.

Leonard et al. (2006) clearly observed this sudden transition in their careful campaign on SN 2004dj (**Figure 7**). The origin and evolution of the polarization of SN 2004dj have been discussed and modeled by Chugai et al. (2005) and Chugai (2006), who conclude that a bipolar ejection of radioactive ^{56}Ni with more mass in the near hemisphere rather than the far hemisphere can account for both the polarization seen in SN 2004dj and the asymmetric profile of the Hα line observed in the nebular phase. Once again, the polarization of SN 2004dj is consistent with a jet-like flow that originates deep in the explosion. The rotation of the polarization position angle may suggest that the nickel is broken into clumps (Leonard et al. 2006); that other composition inhomogeneities disrupt the photosphere (Chugai 2006); that the axis of the jet is tilted with respect to another measure of the geometry in the inner regions, perhaps the rotational axis of the core (see Section 4.5.2); or that a combination of these effects comes into play.

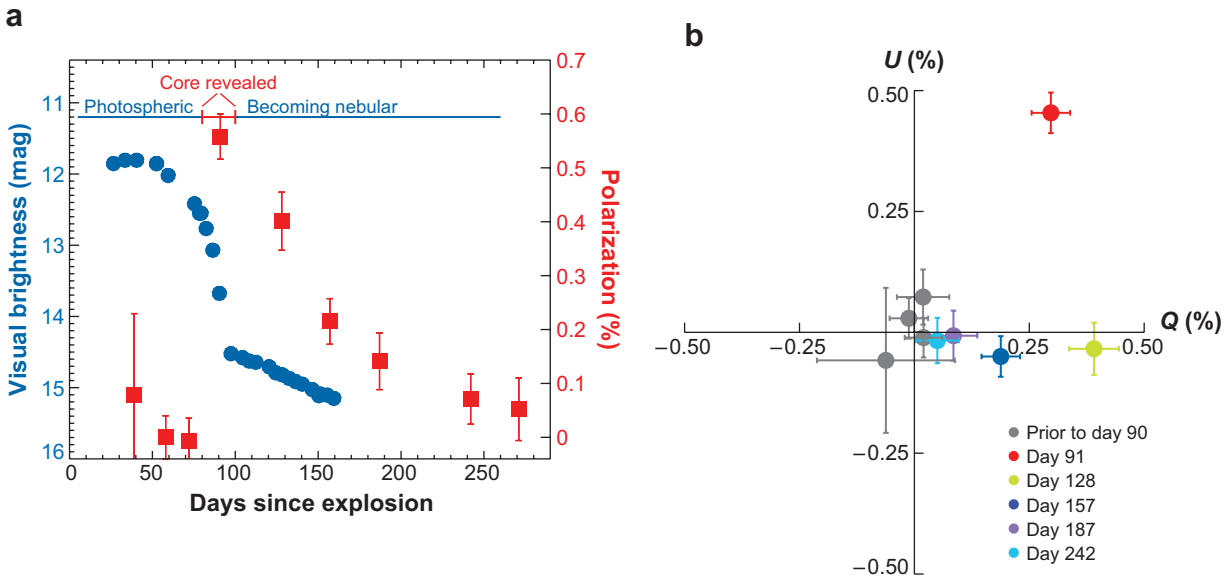

Figure 7

(*a*) Light curve and continuum polarization of SN 2004dj. The red boxes represent the median of the rotated Stokes parameter in the interstellar polarization–subtracted data over the spectral range 6800–8200 Å, showing the dramatic rise in the continuum polarization as the inner core is revealed. The blue circles represent the visual brightness and show the end of the plateau phase and the transition to the exponential tail that is presumed to result from radioactive decay. Figure taken from Leonard et al. (2006). (*b*) Evolution of SN 2004dj with time in the *Q/U* plane from the spike in polarization at 91 days, through the subsequent decline as the ejecta thin out and become optically thin to the scattering that induces the polarization. Note the rotation of the polarization angle between the point at 91 days and the point at 128 days by approximately 30°, after which the angle remains essentially constant. Figure courtesy of D. Leonard.

4.3.2. Type IIn. Type IIn supernovae are characterized by hydrogen-rich ejecta with narrow emission lines (Schlegel 1990) that are attributed to emission associated with substantial circumstellar interaction. The differences in the progenitors and their evolution that distinguish these events from classical Type IIP supernovae are not clear. Spectropolarimetry can provide useful new information to address the issue.

The first Type IIn supernova with spectropolarimetry was SN 1998S. This event was observed by Leonard et al. (2000) approximately 2 weeks before maximum light and by Wang et al. (2001) approximately 10 days and 41 days past maximum light. SN 1998S displayed narrow emission lines characteristic of Type IIn supernovae but also lines characteristic of Wolf-Rayet stars that are not usual for this class. This suggests that SN 1998S had already lost substantial mass from its envelope so that, although interesting, it may not be representative of all Type IIn supernovae. Leonard et al. (2000) favored the interpretation that the broad lines were unpolarized and the narrow lines were polarized. With the benefit of two more epochs of data and the assumption that the ISP does not vary with time, Wang et al. (2001) made a rather different estimate of the ISP, giving a continuum polarization at the first epoch of ∼1.6%. This ISP estimate also implies that both the broad lines and the narrow lines are polarized in the premaximum spectrum, with the continuum displaying an essentially constant position angle. Ten days after maximum, the continuum shows a somewhat smaller polarization, with a rotation of approximately 34° compared to the premaximum data. The polarization then grows to approximately 3% while maintaining the same position angle.

A full analysis of the polarization of Type IIn supernovae must also account for the physical state and geometry of the circumstellar medium (Chugai 2001). Hoffman et al. (2007) showed that Type

TYPE IIb SUPERNOVAE

The Type IIb events are defined as those that show distinct evidence of hydrogen at early times, but then distinct evidence of helium—similar to a Type Ib supernova—at later epochs. These events are believed to have lost all but a very thin layer of hydrogen, probably through transfer to a companion. The binary companion to the prototype Type IIb SN 1993J has been specifically identified (Maund et al. 2004).

IIn SN 1997eg displayed loops in the *Q/U* plane over the Hα line. This implies that the continuum and line-forming regions had different geometries with different orientations. Hoffman et al. (2007) suggest that the ejecta had an ellipsoidal photosphere and that the circumstellar medium in which the hydrogen lines were formed had a flattened disk-like profile. Deeper investigation into this supernova and the polarization of the narrow lines associated with SN 1998S is warranted.

Type IIn supernovae usually show a clear dominant axis. Therefore, they are usually SP Type D0 or D1 in the continuum. Some Type IIn supernovae show loops across spectral lines. Those features would be classified as SP Type L.

4.4. Type IIb: SN 1993J and Similar Events

With regard to whether the asymmetries of core-collapse supernovae are peculiar to individual events or representative of generic phenomena, and whether the asymmetries are associated with the fundamental mechanism of core collapse or peculiarities of the environment, the Type IIb supernovae represent an important test case (see TypeIIb Supernovae sidebar). By examining the Type IIb supernovae, one is intrinsically looking closer at the underlying machine of the explosion. Important issues include whether this class of events displays properties similar to other core-collapse supernovae or properties especially characteristic of their class that might be clues to their origin.

4.4.1. SN 1993J. Doroshenko, Efimov & Shakhovskoi (1995) presented six epochs of UBVRI polarimetry of SN 1993J, spanning the rise and decline associated with the second peak in the light curve (see The Light Curve of SN 1993J sidebar). They found that the U and B data followed a fixed orientation in the *Q/U* plane, but that the longer wavelength data formed arcs or partial loops with time. The authors suggested that the intrinsic polarization may contain two components that have different orientation and time variability. From our current perspective, these remarks seem prescient.

Spectropolarimetry was presented by Trammell, Hines & Wheeler (1993) and by Tran et al. (1997). Both groups assumed that the intrinsic polarization was zero at the peak of the Hα line,

THE LIGHT CURVE OF SN 1993J

SN 1993J showed an initial spike and decline in luminosity attributed to the fireball phase as the shock hit the star's surface and the shocked material rapidly adiabatically expanded and cooled. A secondary peak and a final exponential tail followed, both presumed to have been powered by radioactive decay. The helium lines that mark the class emerged near the second peak. [For an early summary of the polarization data, see Wheeler & Filippenko (1996).]

but differed on their treatment of the underlying continuum. We now recognize that Hα can be blended with He I 6678. This makes the assumption that Hα is unpolarized highly questionable (Maund et al. 2007c). By re-examining the data, employing the constraint that the blue end of the spectrum may be substantially depolarized, we see that Tran et al.'s (1997) ISP estimate appears to be preferable to that of Trammell, Hines & Wheeler (1993), although there are questions regarding the possibility that the polarization angle assigned by Tran et al. may affect the data's interpretation. We also note that Tran et al.'s method to subtract the continuum contribution and fit for the ISP can have significant uncertainties in both the amplitude and angle that they do not assess.

Tran et al. (1997) detected the rotation of the position angle across line features in their latest data, showing that the emission lines of He I, Fe II, and H were intrinsically polarized with position angles that are different from that of the continuum. This also suggests some degree of nonaxisymmetric structure. Their evidence at [OI] is marginal and forbidden lines are not expected to contribute to polarization. The data for SN 1993J displayed in a *Q/U* diagram show little evidence for a dominant angle, but real deviation from zero polarization. SN 1993J is classified as SP Type N1.

4.4.2. SN 2001ig. Maund et al. (2007c) observed the Type IIb SN 2001ig over multiple epochs. They deduced low intrinsic polarization 13 days after the explosion, ~0.2%, consistent with a nearly spherical hydrogen-rich envelope. There is a sharp increase in polarization and a rotation of the polarization angle by 40° by 31 days after explosion, after the hydrogen envelope has become optically thin. At this later epoch, the data conform to a dominant axis and would be classified as SP Type D0. The rotation of the position angle shows that the asymmetry of the second epoch was not directly related to that of the first epoch. As illustrated in **Figure 8**, the most highly polarized lines in SN 1991bg showed wavelength-dependent loop configurations in the *Q/U* plane (see Section 3.5), so these lines, especially He I, are classified as SP Type L. This demands some nonaxisymmetric structure. After SN 1987A, SN 2001ig was one of the first

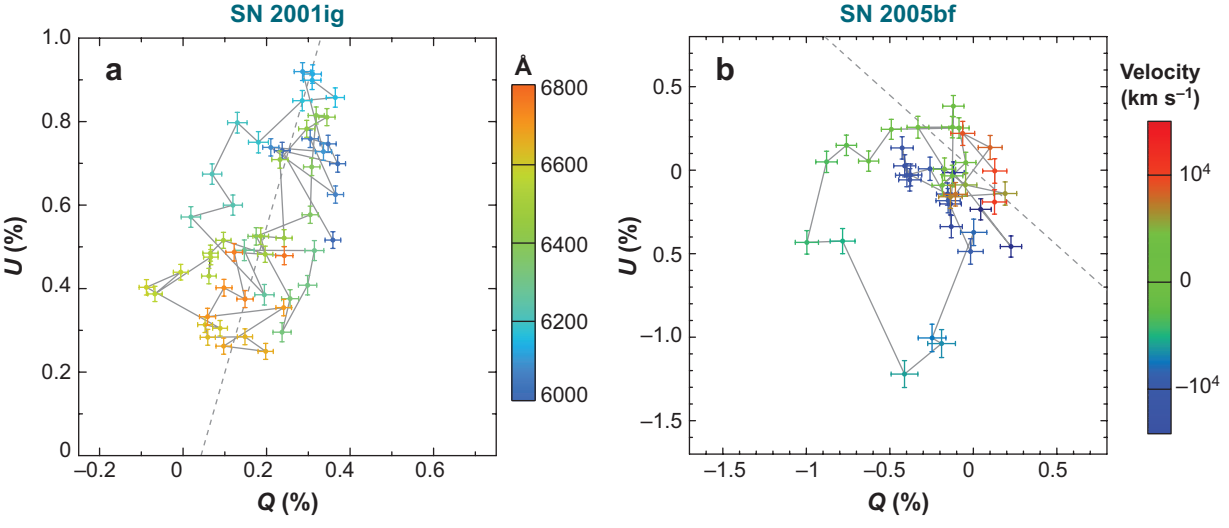

Figure 8

Q/U plane loops, corrected for the relevant interstellar polarization, of He I 6678 Å/Hα in the Type IIb SN 2001ig (*a*) and He I 5876 Å in the Type Ib/c SN 2005bf (*b*). The loops are indicative of nonaxisymmetric structure. Figures taken from Maund et al. 2007b,c.

clear examples of this loop morphology, a characteristic we have come to recognize as generic in core-collapse explosions. We cite other examples throughout this review.

The polarization properties of SN 2001ig are similar to SN 1993J and SN 1996cb but not identical. The observing epochs are not the same and the polarization evolves, so one must be careful when making comparisons. The data suggest that Type IIb supernovae may arise in similar binary systems but may not be so identical that they require an identical observer angle, as suggested by Wang et al. (2001). A further implication is that the class of Type IIb supernovae is not simply an artifact of viewing angle. Spectropolarimetry may thus address an important issue and invites deeper exploration into the nature of the evolution that leads to the progenitors of Type IIb explosions rather than to other types of hydrogen-stripped events. One possibility is that mass transfer in a binary system does not strip the whole hydrogen envelope and that some other process, perhaps a strong stellar wind, is necessary to produce progenitors that are completely stripped of their hydrogen. We explore those sorts of events below.

4.5. Stripped Core (Type Ib and Ic) Supernovae

Type Ib supernovae show strong evidence for helium lines, but scarcely any evidence for hydrogen in the total flux spectra. The total flux spectra of Type Ic supernovae show little evidence for either hydrogen or helium. It is unclear why Type Ib and Ic supernovae have less hydrogen than Type IIb supernovae, how Type Ic supernovae can lose much of their helium as well, and which Type Ic supernovae are connected to gamma-ray bursts. One goal of the continued study of Type Ib and Type Ic supernovae is to seek a deeper understanding of the properties of asymmetry that are common to all core-collapse events and hence to discover important clues on the physical mechanism of the explosion. Spectropolarimetry may also help better explain why some progenitors expel virtually all their hydrogen, whereas others, Type IIb, retain a small amount.

Types Ib and Ic supernovae occur in stars that have already shed nearly all their outer hydrogen layers, allowing a closer look into mechanisms of the exploding star. Wang et al. (2001) discussed how the tendency of these events to show more polarization than Type II supernovae supports an aspherical machinery of the explosion. In this section we explore the data that gave rise to that key conclusion.

4.5.1. SN 1997X. Type Ic SN 1997X was the first event that hinted Type Ic supernovae are more polarized than Type II supernovae, and hence that the machinery of core collapse is intrinsically strongly asymmetric (Wang et al. 2001). SN 1997X showed exceptionally high polarization, as much as 7%. Much of this high polarization resulted from ISP, but the time dependence showed a substantial intrinsic polarization. Wang et al. (2001) suggested that the polarization of SN 1997X may have been as high as 4%. There seems to have been a steep drop in polarization in the first 10 days or so, a factor that requires explanation.

SN 1997X displayed little or no evidence of helium lines in its total flux spectrum, which provided the basis for its classification as a Type Ic supernovae. However, the polarization spectra showed clear spectral features associated with He I λ5876 and λ6678 (**Figure 9**). The helium absorption features peaked at 15,000 km s^{-1}, and the wings reached speeds of 28,000 km s^{-1}. Again, spectropolarimetry is a useful tool to reveal important aspects of the progenitor evolution by more tightly constraining the amount of the helium left and its geometry in the outer layers of the progenitor. The spectropolarimetry supports arguments for a continuum between the Type Ib and the Type Ic spectral classes, rather than a distinct transition between them. In the *Q/U* plane, SN 1997X evolves from an SP Type N1 around maximum to an SP Type D1 approximately 1 month later.

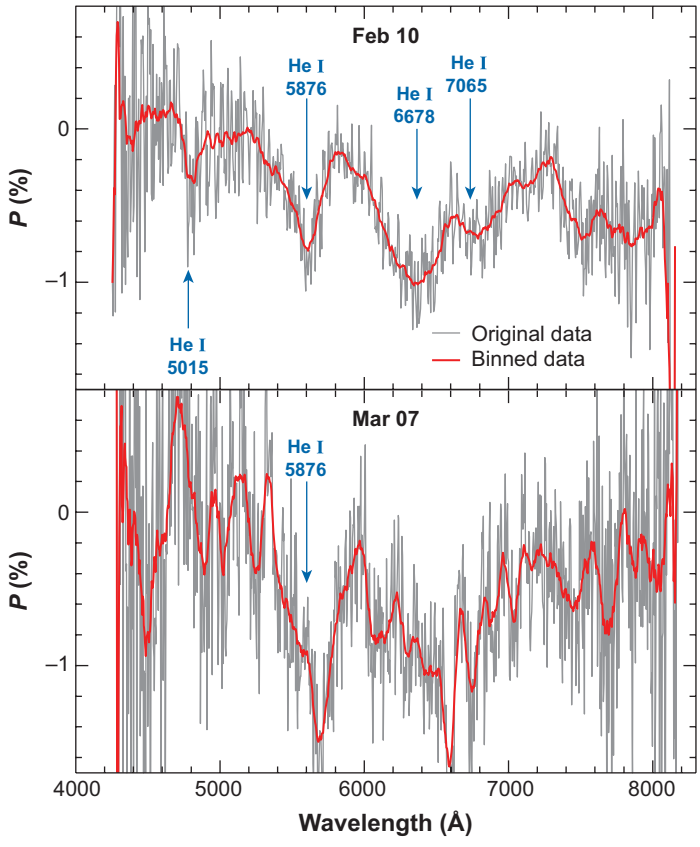

Figure 9

Polarization spectrum of Type Ic SN 1997X on February 10, 1997, and March 7, 1997, approximately 5 days and 30 days after maximum light, respectively. Note the prominent evidence for He I lines in the February 10 spectrum even though this event was otherwise identified as helium deficient. Gray represents original data, red represents binned data. From L. Wang, P. Höflich, and J. C. Wheeler, unpublished.

4.5.2. SN 2005bf. SN 2005bf was an especially interesting example of a Type Ib/c supernova. It had a double-peaked light curve with a first maximum approximately 20 days after the explosion and a second, brighter maximum approximately 20 days later. In addition, it resembled a helium-poor Type Ic in early data, but later developed distinct helium-rich Type Ib features (Tominaga et al. 2005, Folatelli et al. 2006, Parrent et al. 2007). Spectropolarimetry of this event provided the opportunity to look for common aspects of core collapse, clues to the nature of the Type Ib/c spectral classification, and evidence concerning the special nature of SN 2005bf.

Maund et al. (2007b) presented spectropolarimetry of SN 2005bf from May 1, 2005, 34 days after the explosion, 18 days after the first peak in the light curve, and 6 days before the second peak when the supernova was in the Type Ib phase. Although the ISP may have been substantial, intrinsic continuum polarization is still consistent with global asymmetry of the order of 10%. The data tend to fall along a single locus, suggesting a principal axis and jet-like flow, but they also show considerable scatter around that dominant axis. SN 2005bf showed a distinct loop in the He I λ5876 line (**Figure 8**), adding to the evidence for the ubiquity of such features, perhaps especially in helium, and further suggesting a departure from axisymmetry. They observed polarization as

high as 4% in the absorption components of Ca II H&K and the Ca II IR triplet, rivaling that in SN 1997X. The calcium and helium lines showed different polarization distributions in the *Q/U* plane. Iron lines and the prominent O I λ7774 line were not polarized (for a contrasting case, see the discussion of SN 2002ap in Section 4.6). SN 2005bf was classified as SP Type D1 overall and SP Type L in the helium line.

The spectropolarimetry helped to construct a picture of the nature of SN 2005bf that differed from those already in the literature. Maund et al. (2007b) suggested that the progenitor of SN 2005bf comprised a C/O core surrounded by a helium mantle; that is, the progenitor was structurally that of a Type Ib supernovae. The lack of iron polarization suggested that a nickel jet had not penetrated the surface. The lack of O I polarization suggested that the photosphere had not receded into the C/O-rich core. This helium star was presumed to have its own axis of symmetry, probably a rotation axis. To this basic picture, Maund et al. (2007b) added the tilted-jet model in which the jet axis is misaligned with the symmetry axis of the mantle. A possible rationale for this assumption is given by core-collapse models that decouple the spin axis of the proto-neutron star from the spin axis of the progenitor star (Blondin & Mezzacappa 2007). In the tilted-jet model, the continuum polarization arises in the aspherical photosphere. The helium mantle contains a solar abundance of calcium. The calcium thus resides primarily in the photosphere and reflects in part its geometry. Some of the calcium is also subject to the asymmetric excitation owing to the buried nickel-rich jet that has penetrated the C/O core but not the helium mantle. This gives the calcium a different net polarization angle compared to the photosphere. Unlike calcium, helium is only observed owing to excitation of the nickel jet. Because it has no photospheric component, it shows yet again another orientation, that of the jet.

Maund et al. (2007b) suggested that SN 2005bf resembled a Type Ic supernovae early on because the photosphere had not yet receded to a location in which the excited helium could be seen. At a later phase, the excited helium could be seen, and the supernova resembled a Type Ib. The notion that helium might appear at different times in different events has long been discussed (Swartz et al. 1993). SN 2005bf showed again that spectropolarimetry is a valuable probe of the similarities and differences between Type Ib and Type Ic supernovae.

Although the tilted-jet model was designed to qualitatively account for the characteristics of SN 2005bf, its basic features—an asymmetric core that might vary in mass and composition and a tilted jet that carries asymmetric excitation to various depths and at various angles—may help to illuminate other core-collapse events. SN 2008D, being observed as this review was completed, may be another example of an SN 2005bf-like event.

4.6. Polarization of High-Velocity SN Ic and Gamma-Ray-Burst-Related Events

As mentioned in Section 1, the gamma-ray-burst revolution (Woosley & Bloom 2006) unfolded in parallel with the developments in the polarization of supernovae. There is a strong suggestion that spectropolarimetry may also shed light on the supernova/gamma-ray-burst connection as gamma-ray bursts result from jets (Wang & Wheeler 1998). There is a concern that asymmetric explosions could mimic some of the effects of high-velocity activity that has been interpreted as high energy with spherical models (Höflich, Wheeler & Wang 1999). Others have argued that large ejecta energy and nickel mass are needed even if the explosion were asymmetric (Maeda et al. 2002).

The most famous example of a high-velocity Type Ic, SN 1998bw, was apparently associated with the gamma-ray burst of April 25, 1998. Much has been written of this event (van Paradijs et al. 2000), a spectacularly bright supernova and an interestingly dim gamma-ray burst, so we do not summarize that literature here. Patat et al. (2001) presented spectropolarimetry of SN 1998bw

that suggested a moderate intrinsic polarization that might have increased to the red in the earlier data. Few doubt that SN 1998bw was asymmetric. It remains unclear what affect asymmetries had on the spectral and photometric properties.

X-ray-flashes: events presumed to be related to gamma-ray bursts but they show softer radiation outbursts

The Type Ic SN 2002ap represented an especially interesting case. It showed high velocities, but neither a strong relativistic radio source nor excessive brightness. This event convinced many people that the proper nomenclature for this subset of hydrogen- and helium-deficient supernovae should be high-velocity Type Ic, rather than hypernovae. Spectropolarimetry was obtained by Kawabata et al. (2002), Leonard et al. (2002a), and Wang et al. (2003b), covering approximately 6 days prior to maximum light to 30 days after maximum light. The data were especially interesting and complex, showing a shift in the polarization angle of the continuum and different orientation of position angles for oxygen lines, calcium lines, iron lines, and the continuum. This is strong evidence for nonaxisymmetry. SN 2002ap was classified as SP Type D0 in the continuum and SP Type L in strong lines.

The polarized Ca II IR triplet feature appeared later than that of the O I line (Kawabata et al. 2002, Wang et al. 2003b). This behavior is expected if the calcium line is primarily formed in the photosphere and is excited to display an asymmetric geometry only as the ejecta thin out and the outer regions are exposed to the asymmetric excitation of an underlying nickel jet. Wang et al. (2003b) proposed that the jet was still buried in the oxygen mantle in SN 2002ap. A buried jet model might then account for the observations of SN 2002ap with the calcium partaking partly of the photospheric geometry and partly of the asymmetric excitation, as proposed for SN 2005bf (see Section 4.5.2).

SN 2003dh and SN 2006aj are especially interesting as they correspond to the counterparts of gamma-ray burst GRB030329 and the X-ray flash XRF060218, respectively. Kawabata et al. (2003, their figure 1*d*) reported a possible polarization of SN 2003dh at 7000–8000 Å (a region contaminated by sky lines) with a position angle of ∼130°, nearly orthogonal to that of the purported ISP. Because the line of sight was closely along the jet of the gamma-ray burst (presumably a symmetry axis), any polarization would represent nonaxisymmetry.

Maund et al. (2007a) reported a single epoch of spectropolarimetry for SN 2006aj obtained approximately 10 days after the X-ray flash and hence near the estimated maximum of the supernova's light curve. The polarization is nearly 4% in the blue, making SN 2006aj another rival, such as SN 1995bf, to SN 1997X (see Section 4.5.1). This raises the issue as to whether SN 1997X was an X-ray flash. Maund et al.'s (2007a) polarization spectrum is consistent with Gorosabel et al.'s (2006) photometric data and with Kawabata et al.'s (2003) spectropolarimetry of SN 2003dh, in particular the high polarization of oxygen and calcium. Once again the event likely was observed down the jet axis, so the polarization is presumed to result from a breakdown in axisymmetry. SN 2006aj was classified as SP Type L.

4.7. Implications of Polarization for Core Collapse

That the asymmetry of many core-collapse supernovae has a tendency to align in one direction provides an important clue on the engine of the explosion. The mechanism that drives core-collapse supernovae likely produces energy and momentum aspherically from the start and then holds that special orientation long enough for its imprint to be permanently frozen into the expanding matter. Appropriate outflows might be caused by magnetohydrodynamic jets, accretion flow around the central neutron star, asymmetric neutrino emission, magnetoacoustic flux, or some combination of those mechanisms. Another alternative, perhaps intimately related, is that material could be ejected in clumps that block the photosphere in different ways in different lines. Jet-like flows will induce clumping so that these effects go together.

The light we see from a supernova comes substantially from the decay of short-lived radioactive elements ^{56}Ni, ^{56}Co, and later ^{44}Ti in the debris. If this material is ejected in an axial fashion, then the overall debris shell could be nearly spherical, whereas the asymmetric source of illumination leads to a net polarization. This mechanism accounts for the polarization in the early phases of Type IIP supernovae.

By injecting jets of mass and energy along a common axis, typical aspherical configurations emerge. Bow shocks form at the heads of the jets as they plow through the core, and a significant portion of the star's matter bursts through the core along the jet axis. The bow shocks also drive transverse shocks and associated flow sideways through the star. These shocks proceed away from the axis, converge toward the star's equator, and collide in the equatorial plane. From there, matter is compressed, heated, and ejected in an equatorial torus perpendicular to the jets. Models have shown that sufficiently energetic jets can both cause the explosion of the supernova and imprint asymmetries (Khokhlov et al. 1999). Whether jets alone can explain the explosion energetics or whether jet-like flow merely supplements the standard neutrino-driven explosion or some other explosion process remains to be seen. If the jets along the symmetry axes are somewhat unequal, they might also account for the runaway velocities of pulsars and more complex flow patterns in the ejecta. There is a need to understand what happens to the dynamics and shape of ejecta if unequal jets break the mirror symmetry.

4.8. Summary of Core-Collapse Spectropolarimetry

Every major spectral type of core-collapse supernova has now been sampled with spectropolarimetry. They are all polarized and hence substantially asymmetric. This is a general property of core collapse, not the peculiarity of single events. Although each individual supernova has its own properties, basic themes emerge. The fundamental cause of the asymmetry is deep in the ejecta and is a generic property of core collapse. The asymmetry is characterized by a dominant polarization angle, the most straightforward explanation of which is directed flow, a jet. Atop this basic formation, there are significant, composition-dependent structures that signal generic, large-scale departures from axisymmetry. Any physical model of core collapse must address these realities.

5. THERMONUCLEAR SUPERNOVAE

The continuum polarization of Type Ia supernovae tends to be smaller than that for core collapse, but the line polarization can be substantial. The latter is usually only clearly seen in observations prior to maximum light, so the requisite observations are challenging to acquire. Although the sample is small, a broad range of behavior of Type Ia supernovae has been observed. All show substantial asymmetry.

5.1. Normal Type Ia

SN 1996X was the first Type Ia supernova with spectropolarimetry prior to optical maximum and the first that revealed a polarized component intrinsic to the supernova. Wang, Wheeler & Höflich (1997) presented broadband polarimetry and spectropolarimetry of SN 1996X approximately 1 week before and 4 weeks after optical maximum. The Stokes parameters derived from the broadband polarimetry were consistent with zero polarization. The spectropolarimetry showed broad spectral features intrinsic to the supernova atmosphere with a rather low polarization ($\sim$0.3%) identifiable only after careful theoretical modeling. The spectral features in the polarized spectrum of SN 1996X were richly structured and did not show strong correlation with the features in the

total flux spectrum. The authors noted that, because the polarization spectrum is formed at the composition-dependent (and hence wavelength-dependent) last-scattering surface, the polarized flux should show a higher degree of wavelength dependence than the multiply scattered, blended total flux spectrum. Model calculations showed that the polarization could be produced by electron scattering and scattering from blended lines. The models suggested that the polarization was formed at the boundary between the partially burned silicon layers and the inner iron-peak layers. No other Type Ia supernova with early spectropolarimetry has shown a polarized spectrum quite like SN 1996X. The SP Type of SN 1996X is N1.

Leonard et al. (2005) presented spectropolarimetry of SN 1997dt approximately 21 days after maximum light. This object did display distinct line polarization in Fe II and Si II, so some of the polarization is intrinsic, but the amount remains uncertain. As shown below, the polarization of Type Ia supernovae at this later phase tends to be quite low.

5.1.1. SN 2001el: high-velocity Ca II IR triplet. The first detailed, high-quality, time-sampled spectropolarimetry of a core-normal Type Ia supernova (Branch et al. 2006) was obtained for SN 2001el (Wang et al. 2003a) (**Figure 10**). The degree of polarization in the continuum and across spectral lines decreased sharply 10 days after optical maximum and became undetectable approximately 19 days after optical maximum. Prior to optical maximum, the linear polarization of the continuum was ∼0.2%–0.3% with a constant position angle, showing that SN 2001el had a well-defined axis of symmetry. Significant deviations orthogonal to the dominant axis suggested that the continuum was SP Type D1. The Si II λ6355 line showed a broad loop on the *Q/U* diagram and is thus classified as SP Type L across that wavelength range. The polarization was nearly undetectable 1 week after optical maximum. These data showed that the temporal behavior of Type Ia supernovae was the reverse of core-collapse events. It is the outer layers of Type Ia supernovae that are especially asymmetric, not the inner layers.

SN 2001el also gained fame because it was the first Type Ia supernova in which the strong high-velocity (20,000–26,000 km s^{-1}) component of the Ca II IR triplet was observed as a feature clearly separated from the photospheric calcium feature. Hatano et al. (1999) identified this high-velocity feature for SN 1994D, but it was much weaker there. The high-velocity Ca II has proven nearly ubiquitous in subsequent studies (Mazzali et al. 2005). This high-velocity component showed much higher polarization than the continuum (∼0.7% versus 0.2%–0.3%, respectively) and a different position angle. Because the position angle varies across the line, the high-velocity Ca II showed a distinct loop on the *Q/U* plane, making this feature a dramatic example of an SP Type L (see **Figures 2** and **10**). The polarization spectrum of SN 2003du obtained by Leonard et al. (2005) 18 days after maximum was virtually identical to that of SN 2001el at a comparable phase, evidence that this behavior is not isolated to a single rare event. Kasen et al. (2003) showed that the loop in the high-velocity Ca could be accounted for by a clumpy shell or a torus with sufficiently high optical depth (see **Figure 2**).

Spectropolarimetry of SN 2004S (Chornock & Filippenko 2006) showed that the high-velocity component of Ca II IR was not highly polarized, although the corresponding position angle was rotated with respect to that of the continuum. The relatively late phase (9 days after maximum light) lends a cautionary note as to the significance of the low polarization. The behavior of SN 2004S is consistent with that of SN 2001el and shows the importance of acquiring early observations of Type Ia supernovae.

5.1.2. High-velocity photospheric lines. Another important event was SN 2004dt, for which Wang et al. (2006) obtained data approximately 7 days before maximum light and Leonard et al. (2005) did so approximately 4 days after maximum light. Although nominally a normal Type

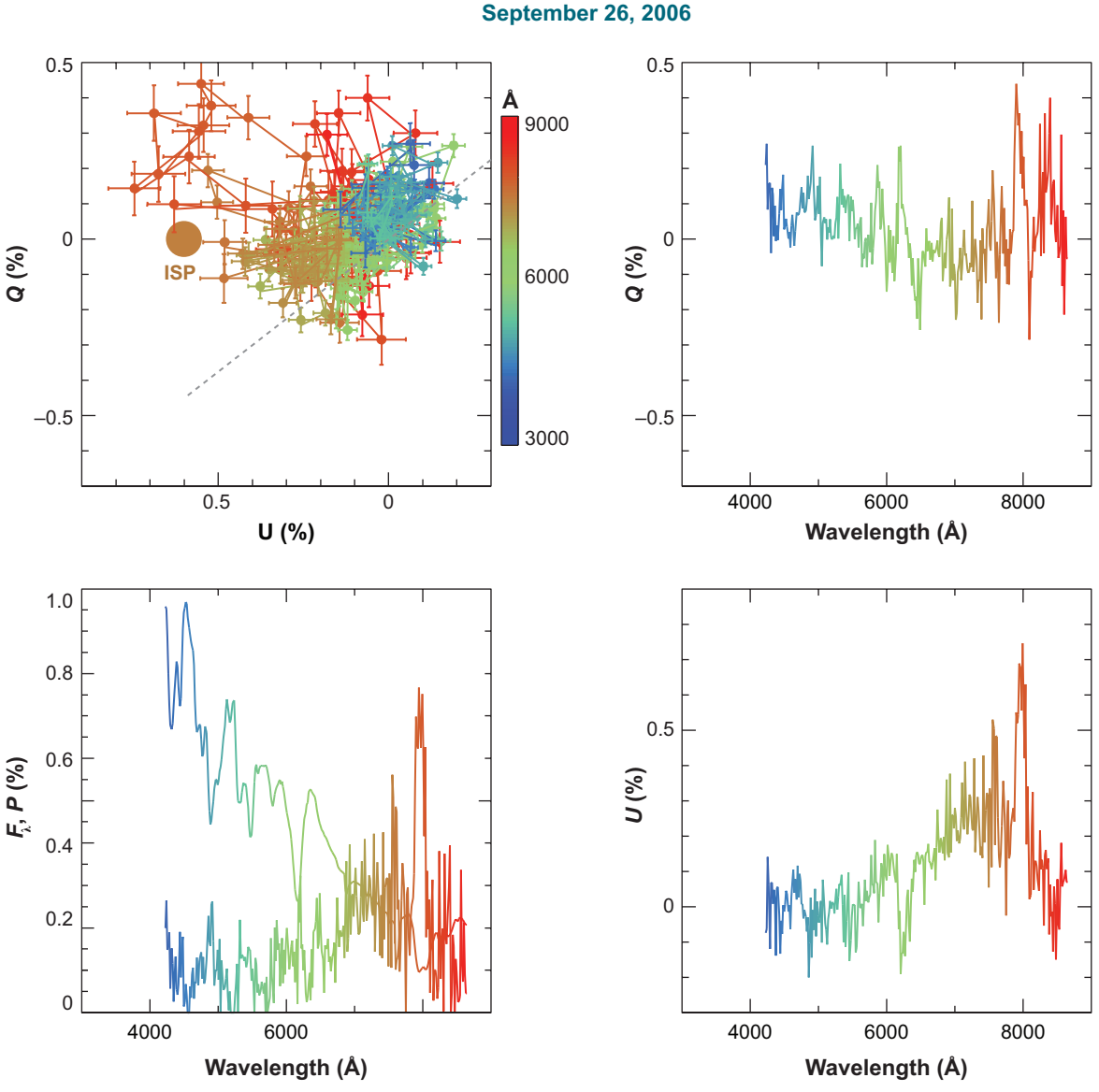

Figure 10

Spectropolarimetry of Type Ia SN 2001el on September 26, 2001, 7 days before maximum. The assumed interstellar polarization is shown as a solid brown dot in the *Q/U* plot (*upper left panel*). The straight line illustrates the dominant axis shifted to the origin of the *Q/U* plot. The *Q* (*upper right panel*) and *U* (*lower right panel*) spectra show conspicuously polarized spectral features. The flux spectrum is also given in the lower left panel as the line rising to the left. The lower left panel shows the correlations of the degree of polarization and the spectral features. The high-velocity Ca II IR feature is especially prominent at 8000 Å. Figure taken from Wang et al. (2003a).

Ia in terms of its light curve, SN 2004dt falls in a subclass of events that show especially high photospheric velocities (as opposed to the high-velocity separated Ca II IR lines of SN 2001el). This category was discussed by Benetti et al. (2004, 2005) as the high-velocity gradient class and by Branch et al. (2006) as the broad-line class.

SN 2004dt also had a distinct polarization spectrum. The variation of the polarization across some Si II lines approached 2%, putting SN 2004dt among the most highly polarized SN Ia. Unlike SN 2001el, the polarization of the Ca II IR features was prominent for SN 2004dt, but the polarization levels of the Si II lines were the strongest.

Leonard et al. (2005) also presented data on SN 2002bf at approximately the same postmaximum time as for their data on SN 2004dt. Ca II is prominent with a polarization of ∼2%, with Si II rather modest in the dominant axis. The orthogonal projection shows the Si II line distinctly, with perhaps a hint of O I. The data on SN 2002bf are thus tantalizingly different than those of SN 2004dt. Other members of the high-velocity-gradient subclass with spectropolarimetry showing strong polarization of Si II are SN 1997bp and SN 2002bo (Wang et al. 2006).

An especially distinct feature of SN 2004dt was that, in contrast to the strong polarization of Si II, the strong line of O I at 7774 Å showed little polarization signature along the dominant axis defined by the continuum polarization and by the strong Si II λ6355 line (**Figure 11**). Despite the large evolution in the flux spectrum of SN 2004dt between Wang et al.'s (2006) premaximum observations and Leonard et al.'s (2005) postmaximum observations 11 days later, there was relatively little evolution of the polarized spectrum; the Si II and Ca II IR triplet remained significantly polarized, and O I was not.

The SP types across different spectral lines vary for SN 2004dt (**Figure 12**). Owing to the high-quality data from ESO's Very Large Telescope, the observational errors of SN 2004dt could be determined well enough to enable quantitative studies of the *Q/U* diagram of SN 2004dt. The Si II lines and the Ca II IR triplet can be classified as SP Type D1, showing distinct dominant axes but with significant dispersion orthogonal to the dominant axis. The Mg II line is classified as SP Type D0, in which the *Q/U* diagram can be well fitted by a straight line. The O I line shows no dominant axis, but has significant dispersion that is too large to be explained by observational errors, and is thus classified as SP Type N1. We note that no significant looping is found for the lines. This is consistent with a low continuum polarization or only a moderate departure from spherical symmetry of the ejecta.

The degree of polarization in SN 2004dt points to a silicon layer with a substantial departure from spherical symmetry. A geometry that would account for the observations is one in which the distribution of oxygen is on average essentially spherically symmetric, but with protrusions of intermediate-mass elements within the oxygen-rich region. The central regions of SN 2004dt are essentially spherical and consist of fully burned iron-group elements. The distribution of magnesium, of SP Type D0, shows a well-defined symmetry axis and rather smooth geometry (see **Figure 1**) when compared with the distribution of silicon and calcium. The prominent dominant axis of SN 2004dt in silicon, calcium, and magnesium may result from an off-centered ignition (Livne 1993, 1999; Gamezo, Khokhlov & Oran 2004; Plewa, Calder & Lamb 2004; Livne, Asida & Höflich 2005; Röpke, Woosley & Hillebrandt 2007; Plewa 2007) or may be somehow related to the progenitor system.

Leonard et al. (2005) pointed to the simulations of Travaglio et al. (2004), who used significant unburned carbon and oxygen as a basis for interpretation. As stressed by Wang et al. (2006), oxygen has the same velocity profile as silicon in the total flux spectrum, inconsistent with Travaglio et al.'s (2004) model, in which the silicon remains interior to the unburned oxygen. Wang et al. (2006) discuss the inconsistencies of their observations with pure deflagration models that leave substantial unburned carbon and oxygen.

Another well-studied event of the high-velocity-gradient kind is SN 2006X. This event provided the first distinct evidence for a circumstellar medium near a normal Type Ia (Patat et al. 2007). F. Patat et al. (manuscript in preparation) report eight epochs of spectropolarimetry of SN 2006X prior to maximum light and one epoch approximately 40 days later. The polarization of SN

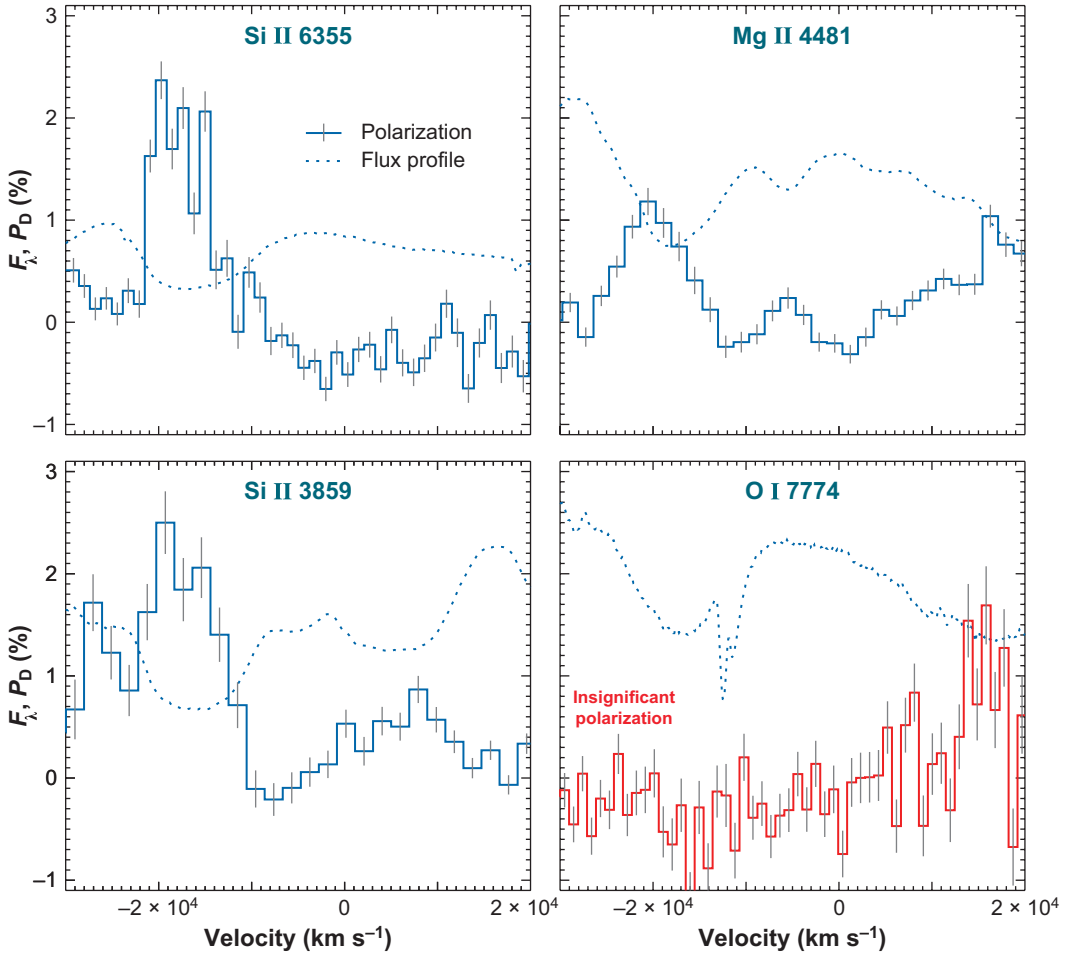

Figure 11

Polarized line features in SN 2004dt. Absorption features in the total flux spectrum and the polarization profiles along the dominant axis are given as a function of velocity for (*clockwise from the upper left*) the lines of Si II λ6355, Mg II λ4481, O I λ7774, and Si II λ3859. The dotted lines give the total flux profiles, whereas the solid lines give the polarization. Note that there is significant polarization in all lines except O I. Figure taken from Wang et al. (2006).

2006X uncorrected for ISP shows a linear decline from approximately 8% at 4000 Å to approximately 2% at 8000 Å. This cannot easily be fit with a Serkowski law, implying that the dust around SN 2006X does not have the same constitution as the average dust in our galaxy. In the earliest data, 10 days before maximum light, the Ca II IR line is strongly polarized (∼1.5%) and the Si II is less so (∼0.5%). As the peak is approached, the Ca line gets less polarized, whereas the Si line gets more polarized. Especially interesting is that the Ca polarization seems to be stronger at +39 days than it had become at day −1. This may result from seeing the inner, clumpy, calcium-rich layers. No other SN Ia has been observed at this epoch with this level of S/N ratio, so it is not known if this is a common property, calling for more late-time observations. Overall, SN 2006X seems to be intermediate in its polarization properties between SN 2001el and SN 2004dt. Similar to SN 2004dt, SN 2006X shows little or no polarization of the O I line, less than 0.3%. The continuum shows a reasonably well-defined dominant axis in the *Q/U* plane, but with significant, and probably

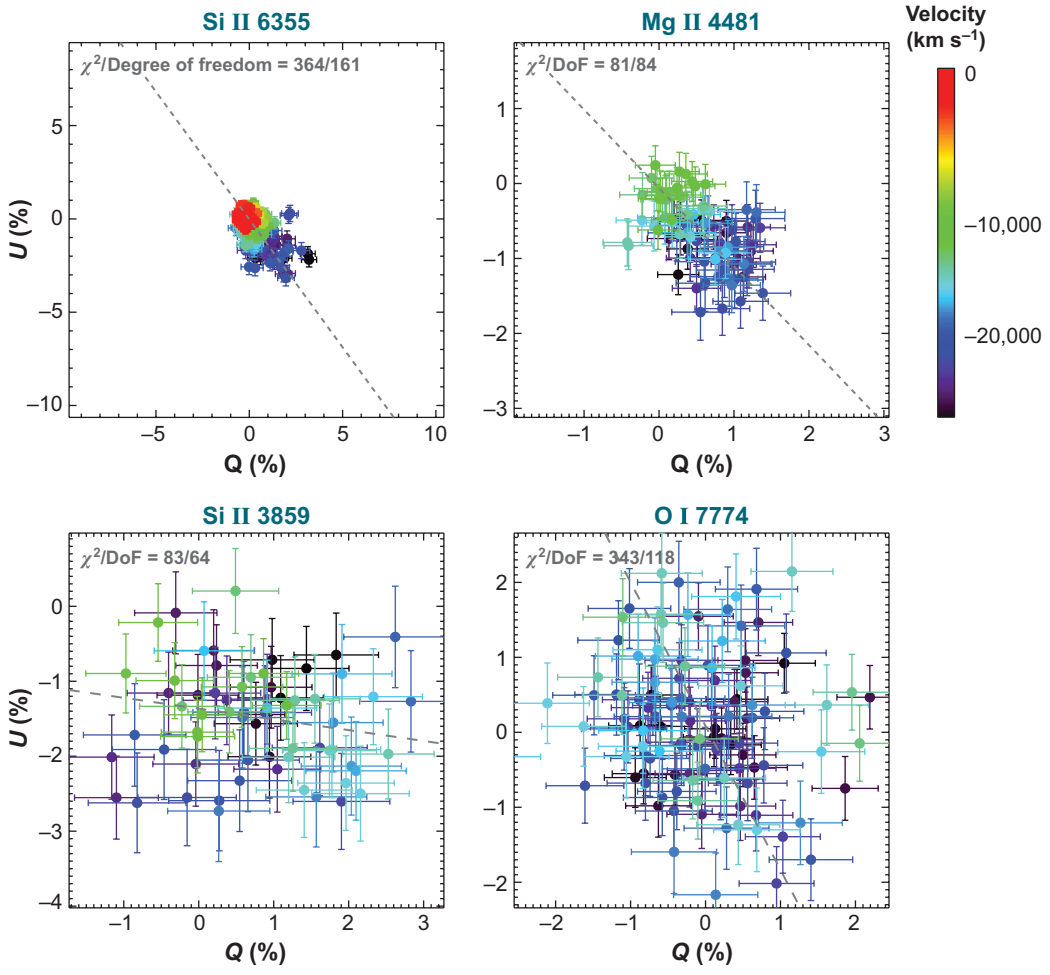

Figure 12

Q/U diagrams of the strongest lines in SN 2004dt and the corresponding linear fits (*dashed lines*): Si II λ6355 (*top left panel*), Mg II λ4481 (*top right panel*), O I λ7774 (*bottom right panel*), and Si II λ3859 (*bottom left panel*). The range of the data points is −25,000 to −10,000 km s^{-1} for these lines. Only the Mg II line is consistent with a straight line, indicating a simple axially symmetric geometry with no detectable clumping. Figure taken from Wang et al. (2006).

real, departures. SN 2006X suffers strong interstellar reddening, and the dust responsible for the reddening likely is distributed close to the supernova (Wang, Baade & Patat 2007).

Interestingly, all the high-velocity Type Ia supernovae show strong polarization, and many show strong dust extinction. The interpretation of the polarization data for these supernovae may be complicated by the presence of dust particles around the supernova (Wang 2005).

5.2. Polarization of Subluminous Type Ia

Another class of Type Ia that can be studied with spectropolarimetry includes those in the low-luminosity category, the prototype of which is SN 1991bg. SN 1999by, observed by Howell et al. (2001), is a nice example of a subluminous Type Ia supernova. The continuum polarization was substantial (0.3%–0.8%) and rose toward the red as predicted by models in which the line-scattering

depolarization is less in the red. The data show a distinct locus in the *Q/U* plane, indicating a favored orientation of the geometry, and hence an SP Type D0 classification. It is not clear whether this is a distinguishing characteristic of subluminous Type Ia supernovae. Howell et al. (2001) speculate that the relatively high well-oriented polarization might be the signature of rapid rotation or binary merger characteristic of subluminous events. They note that for core normal Type Ia, the photosphere should be near the inner iron-rich layers near maximum light and that these iron lines should affect the spectrum. For a subluminous event such as SN 1999by near maximum, the photosphere is expected to be in the silicon layers dominated by continuum scattering.

5.3. The Extremes of Type Ia

Some supernovae show features that characterize them as Type Ia, but other features that are markedly different than the majority of Type Ia. Spectropolarimetry can help to reveal the nature of these rare events.

5.3.1. The hybrid nature of SN 2002ic. SN 2002ic showed distinct evidence for narrow-line hydrogen emission, similar to Type IIn, indicating strong circumstellar interaction but with an underlying spectrum similar to a Type Ia supernova (Hamuy et al. 2003). SN 2002ic thus belongs to an interesting subclass of Type Ia supernovae that have managed, by some circumstance, to explode in a region still rich in hydrogen [see the discussion of SN 2006X above and Gerardy et al.'s (2004) discussion as to whether the high-velocity Ca II feature represents a swept-up hydrogen shell]. Hamuy et al. (2003) conclude that the progenitor system contained a massive asymptotic-giant-branch star that lost several solar masses of hydrogen-rich gas before the supernova explosion.

Wang et al. (2004) obtained spectropolarimetry of SN 2002ic nearly 1 year after the explosion. This is the latest phase of any supernova for which polarization has been positively detected. At this phase, the supernova had become fainter overall, but the Hα emission had brightened and broadened dramatically compared with earlier observations. The spectropolarimetry showed spectropolarization properties typical of Type IIn supernovae and indicated that the hydrogen-rich matter was highly aspherically distributed. Wang et al. (2004) argued that the narrow peak and broad wings of the Hα line and the increase in the strength of Hα with time may be produced by electron scattering in a shocked-heated nebular torus. Chugai & Chevalier (2007) modeled the observed polarization in more detail and concluded that a moderate degree of asymmetry with the major axis approximately 40%–50% longer than the minor axis is sufficient to explain the polarization data. The amount of asymmetry deduced by Chugai & Chevalier (2007) represents the minimum level of asphericity required to explain the data, and the level is still significant. The observations are consistent with a solar mass of clumpy material extending to $\sim 3 \times 10^{17}$ cm, suggesting that the supernova exploded inside a dense, clumpy, disk-like circumstellar environment reminiscent of a proto-planetary nebula.

5.3.2. SN 2002cx and SN 2005hk: weird type Ia? SN 2002cx and SN 2005hk were labeled as very peculiar Type Ia supernovae, showing low peak luminosity, slow decline, high ionization near maximum light, and an unusually low expansion velocity of only approximately 6000 ks s^{-1} (Li et al. 2003, Chornock et al. 2006, Jha et al. 2006, Phillips et al. 2007). The low peak luminosity and slow expansion have been interpreted as possible evidence for an explosion by pure deflagration. Models predict such an explosion to burn less of the white dwarf and to produce less nickel to power the light curve, but in published models this should lead to a significant amount of unburned carbon and oxygen, for which there is little evidence.

Chornock et al. (2006) presented spectropolarimetry approximately 4 days before the maximum light of SN 2005hk. They found that the continuum was polarized approximately 0.4% in the red with a single axis of symmetry dominating the geometry, but with considerable scatter. They also identified a weak modulation of the polarization of the Fe III line at 5129 Å. They argued that the fairly large continuum polarization and lack of strong line features do not correlate with Kasen et al.'s (2004) predictions of the model for a Type Ia supernova viewed down the hole carved by a binary companion in the supernova ejecta (Marietta, Burrows & Fryxell 2000). SN 2002cx, SN2005hk, and their kin still defy consistent explanation.

5.4. The Polarization of the Si II 6355-Å Lines

The Si IIλ6355 line of Type Ia supernovae is one of the strongest lines in the optical range. Wang, Baade & Patat (2007) reported polarization data of 17 Type Ia and compared the degree of polarization across the Si II 6355 Å line to the light-curve properties of the supernovae. **Figure 13** shows the general trend that supernovae with a faster light-curve decline rate past

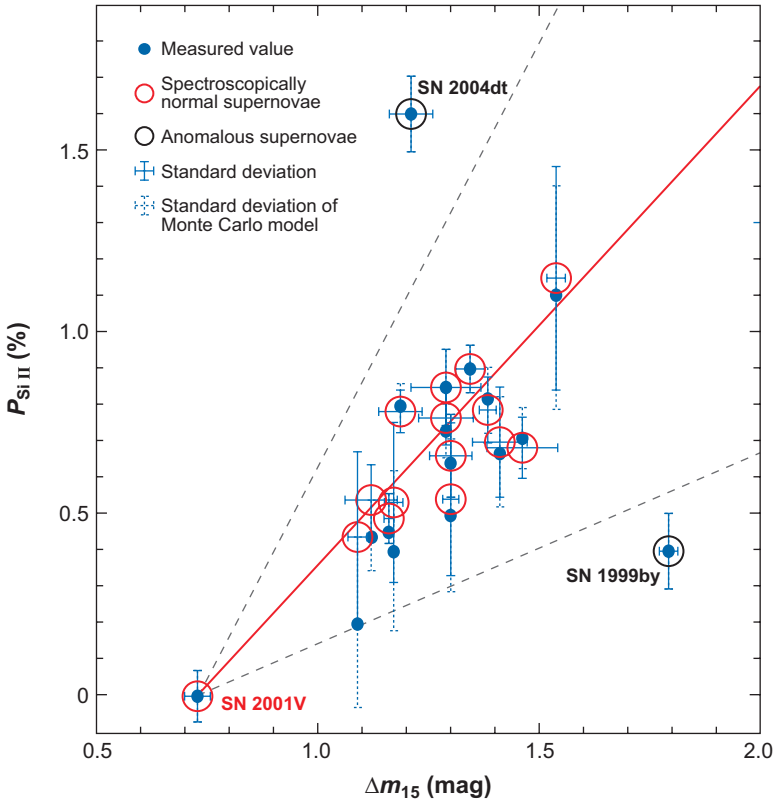

Figure 13

The correlation between the degree of polarization across the Si II λ6355 line and the light-curve decline rate, Δm_{15}, for a sample of 17 Type Ia supernovae corrected to 5 days before maximum. The linear fit represented by the straight red line includes only spectroscopically normal supernovae (*red open circles*). The black open circles show the highly polarized event SN 2004dt and the subluminous SN 1999by. The dashed gray lines illustrate the 1 σ level of the intrinsic polarization distribution around the most likely value for a Monte Carlo simulation with 20 identical opaque clumps of Si II. Figure taken from Wang, Baade & Patat (2007).

optical maximum tend to be more highly polarized. The correlation shows a large dispersion owing to observational noise, but the correlation appears to be significant. The linear fit gives $P_{SiII} = 0.48(\pm 03) + 1.33(\pm 15)(\Delta m_{15} - 1.1)$, where Δm_{15} is the magnitude decline from peak 15 days after *B*-band maximum. The supernova showing the highest polarization across the Si IIλ6355 line is SN 2004dt, which does not follow the linear fit.

Because the continuum polarization is low for all these supernovae, the overall structure of Type Ia supernovae clearly must be rather spherical. This provides a nice check of the use of Type Ia as a standard luminosity source for cosmological studies.

If we accept Δm_{15} as a measure of the brightness of Type Ia supernovae (Phillips 1993), and that brighter Type Ia have a larger amount of ^{56}Ni, we can conclude that supernovae with lower polarization have gone through more complete nuclear burning. This may be reasonable because more complete burning tends to destroy more inhomogeneities and thus makes more spherical supernovae.

5.5. The Implications of Polarization for Thermonuclear Explosions

Wang, Wheeler & Höflich (1997) presented the first polarization models of Type Ia supernovae, which were based on ellipsoidal variations of one-dimensional thermonuclear combustion models. Kasen et al. (2003) presented models of SN 2001el that explored the polarization properties, especially of the high-velocity Ca II IR triplet that was highly polarized with a different polarization angle than the rest of the spectrum. Kasen et al. (2003) investigated the nonaxisymmetric geometries necessary to produce loops in the *Q/U* plane. A clumped-shell model did an especially good job of accounting for the features of the loop defined by the high-velocity Ca II IR line (see **Figure 2** for an example of this sort of calculation), but such models remain phenomenological. A deeper understanding remains elusive.

In the context of various models, Wang et al. (2006) discussed the challenging observations of SN 2004dt that showed polarized magnesium, sulfur, and silicon, but nearly unpolarized oxygen. This is puzzling because models predict that these elements should be intermixed in the outer layers of the explosion and hence might be expected to share geometry. One important class of models includes deflagration models in which the burning is driven only by subsonic turbulent flames that produce irregular structure but do not burn the entire C/O white dwarf (Reinecke, Hillebrandt & Niemeyer 2002; Gamezo et al. 2003; Röpke et al. 2007). Wang et al. (2006) concluded that, although turbulent deflagration models might produce the observed clumpy composition structure, they have difficulty producing the kinematics of the ejecta, especially the high-velocity, yet asymmetric, silicon. Another important class of models includes the delayed-detonation models (Khokhlov 1991) in which the burning starts as a turbulent, subsonic flame, but there is a presumed transition to a supersonic, shock-driven detonation. These models provide good fits to light-curve and spectral data and account for the energetics. Delayed-detonation models burn the outer layers to intermediate mass elements, but are unlikely to generate a turbulent silicon layer as apparently observed in SN 2004dt (Boisseau et al. 1996, Gamezo et al. 1999). Off-center delayed-detonation models (Livne 1999; Gamezo, Khokhlov & Oran 2004; Livne, Asida & Höflich 2005; Röpke, Woosley & Hillebrandt 2007) can yield off-center nickel and off-center, clumpy silicon that may contribute to the induction of polarization (Chugai 1992, Höflich 1995, Höflich et al. 2006), but no completely satisfactory model exists for the polarization of SN 2004dt.

A related possibility is the gravitationally confined detonation model (Plewa, Calder & Lamb 2004) or detonating failed deflagration model (Plewa 2007) in which a plume of burned matter floats to the surface and across the surface of the star to converge at the point opposite from the location at which the plume emerges. The resulting rapid compression of the unburned

material is proposed to trigger a detonation. Kasen & Plewa (2007) have explored this type of model in some detail. They generated synthetic broadband optical light curves, near-infrared light curves, color evolution curves, full spectral time series, and spectropolarization of the model, as seen from various viewing angles. They also compared the statistical properties of the model to observations and commented on orientation effects that may contribute to photometric and spectroscopic diversity. Kasen & Plewa (2007) remarked that their model, although based on a particular physical scenario, may be characteristic of a general class of asymmetric models. They did not attempt to compare their model to a particular supernova, but their total flux spectra do not give a significant O I line; hence their model does not correspond directly to SN 2004dt.

5.6. Summary of Type Ia Spectropolarimetry

Type Ia supernovae are more polarized in the outer layers than in the inner layers, giving an important clue on the nature of their thermonuclear burning. The continuum polarization is low, showing that the explosion is nearly spherical, but the line polarization can be very strong. The line polarization may correlate with the velocity measured from absorption line minimum (Leonard et al. 2005). Some Type Ia supernovae show significant orientation with a dominant axis, but it is not clear whether this correlates with other properties, for instance, the light-curve decline rate. The future holds great promise for the use of spectropolarimetry of Type Ia supernovae to explore the asymmetries of the explosion, the nature of the progenitor system (which should be intrinsically asymmetric), and the nature and geometry of the circumstellar medium.

6. CONCLUSIONS

Höflich et al. (1996) argue that, to some order, the flux spectra of aspherical models can be reproduced by the appropriate adjustment of the parameters of spherical models (e.g., the radius of the photosphere, the density gradient, or perhaps some microturbulence) so that it is difficult to deduce the geometry from the early time flux spectra of supernovae. Certainly flux spectra are mute to important aspects such as different orientations for different chemical species and loops in the *Q/U* plane. Nebular spectra may be more useful indicators of asymmetry because line profiles can reveal velocity asymmetries and small-scale clumping structure, but again, there is no information on the relative orientation of different chemical species.

The totality of the evidence derived from spectropolarimetry of core-collapse supernovae is that the primary driver of asphericity exists deep in the explosion process and that the explosion process often aims at a certain direction in space. Something resembling jet-like flow is strongly suggested. Application of SN II to measurements of the distance scale needs to be considered with care because even asymmetric luminosity sources in the plateau phase can give a small direction dependence to the luminosity (Chieffi et al. 2003).

As summarized here, recent work has revealed that departures from axisymmetry are also ubiquitous in core-collapse supernovae. More work needs to be done to quantify this significant clue to their physics and dynamics. Two basic means to induce asphericity come from a distortion of the progenitor and a jet-like flow that can induce asphericity in both the density structure and the ionization structure. Jet-like flow likely induces significant nonaxisymmetric hydrodynamic instabilities: Rayleigh-Taylor, Kelvin-Helmholz, and Richtmyer-Meshkov (Wheeler, Maund & Couch 2008). A nonaxisymmetric geometry could also be achieved if the jet-like flow were tilted with respect to the progenitor geometry. There are physical reasons why the rotation axis of a newly born neutron star (and hence, presumably, the jet) could differ from the rotational axis

of the progenitor. The jet could also penetrate to different depths in different circumstances, providing considerable variety. In addition, clumps of different density or composition could cause or contribute to the nonaxisymmetry. Ultimately there is also a need to understand the origin of such clumps, with the jet being a potential principal source.

The characteristics of high-velocity Type Ic may result from orientational effects in a mildly inhomogeneous set of progenitors, rather than requiring an excessive total energy or luminosity. When analyzing asymmetric events with spherically symmetric models, one should probably refer to isotropic equivalent energy, luminosity, ejected mass, and nickel mass. The discovery that routine core-collapse supernovae are aspherical and jet-like in turn may provide new insights into more exotic jet-induced events such as gamma-ray bursts and X-ray flashes. We desperately need more high-quality spectropolarimetry of stripped-core events. This has proved difficult in practice, but the few that have been observed have been exceedingly interesting.

The asymmetries observed in Type Ia supernovae may finally yield direct observational evidence for their occurrence in binary systems, as long assumed, and clues to the combustion mechanism. At the time of this writing, there is no fully acceptable model of the origin of the composition-dependent aspherical structure of Type Ia supernovae, certainly not the possible variation of that structure within the distribution of other observed properties of Type Ia supernovae. In particular, neither pure deflagration models, delayed-detonation models, nor gravitationally confined detonation models fully account for the observations. On the contrary, the spectropolarimetry has offered a new tool by which to characterize the nature of the explosion. As the sample grows, we should more deeply understand the nature of the explosion and how it varies among the normal, luminous, and subluminous Type Ia supernovae, and among the high-velocity gradient, broad-line, low-velocity, and other subgenres of the species, such as the hydrogen-rich SN 2002ic and the especially weird SN 2002cx. The seemingly ubiquitous, substantially polarized high-velocity Ca II feature is an especially important aspect to explore with spectropolarimetry. Understanding these asymmetries may be necessary to properly interpret future data on cosmologically distant Type Ia supernovae.

This topic is still in a data-driven phase, but there has been much excellent work for a foundation of understanding (Jeffery 1989, 1990, 1991a; Höflich 1991; Chugai 1992, 2001, 2006; Kasen et al. 2003; Höflich et al. 2006; Kasen, Thomas & Nugent 2006). Much of the basic understanding of the possible behavior of polarized supernovae, especially of the continuum, has been elucidated in terms of ellipsoidal models (Höflich 1991, 1995; Höflich et al. 1996). Prolate models tend to require a larger distortion than oblate models to produce the same net polarization (Höflich et al. 1996). The true geometry, of course, may be some combination of oblate and prolate and may be more complex than what is captured easily by ellipsoidal structures.

Exploring more complex structures requires more general models. Monte Carlo radiative transfer models are most likely to provide the needed generality of the underlying geometry and have the capacity to handle the associated radiative transfer with a realistic amount of computing time. Contemporary examples of these models are the HYDRA code (Höflich 2005) and the SEDONA code (see Kasen, Thomas & Nugent 2006), which have been applied to a number of problems, especially those associated with Type Ia supernovae. These codes treat aspherical geometries, gamma-ray deposition, and line and continuum transfer. They can compute models for the light curves and for the spectral and polarimetric evolution as observed from arbitrary viewing angles.

There are two ways to approach the analysis of polarization data. One is the solution of the forward problem for which a dynamical model is proposed or simulated and the polarimetric evolution is computed to compare with observations. The solution of the backward problem consists of proceeding from the observed data to deduce the geometry of the ejecta. In practice, progress will be made by a process of iteration between these two techniques. Codes such as

these will play a vital role in this iteration. This phase of supernova polarimetry research is just beginning, but holds great promise as the database expands.

SUMMARY POINTS

Spectropolarimetry of supernovae is still a young field, but a number of basic conclusions have important implications for the future of supernova research.

1. Spectropolarimetry has now been obtained for every major spectral type of supernova: Type IIP, Type IIn, Type IIb, Type Ib, Type Ic, and Type Ia of various luminosity classes and peculiarities (**Table 1**). They are all polarized and hence aspherical in some significant way.
2. Presenting the data in the *Q/U* plane as a function of time, wavelength, and especially across individual spectral lines is a powerful way to facilitate its analysis. Spectropolarimetric (SP) types can be assigned based on the distribution of data in the *Q/U* plane.
3. Core-collapse supernovae reveal larger asymmetry as observations are made deeper in the ejecta, either as the ejecta thins with expansion or the progenitors have less massive hydrogen envelopes, showing that the explosion mechanism itself is strongly asymmetric.
4. Type Ia supernovae display modest continuum polarization but very strong line polarization prior to maximum light. The polarization declines after maximum. This is firm evidence that the outer portions of the ejecta are especially significantly aspherical.
5. Core-collapse supernovae routinely show evidence for strong alignment of the ejecta in single well-defined directions, suggesting a jet-like flow. They often show a rotation of the position angle with time of 30°–40°, indicating a jet of material emerging at an angle with respect to the rotational axis of inner layers.
6. Spectropolarimetry is an especially sensitive tool to study the presence and asymmetry of helium that is excited by nonthermal processes associated with radioactive decay. The helium, in turn, is an important clue to the nature and extent of mass loss from the progenitor; to the relations between Type IIb, Type Ib, and Type Ic supernovae; and to the asymmetric distribution of the radioactive elements.

FUTURE ISSUES

1. Core-collapse supernovae frequently display loops in the *Q/U* plane that indicate significant and systematic departures from the predominant axisymmetric structure. This asymmetry must be understood in terms of physical models.
2. Large-scale asymmetries in the outermost high-velocity portions of the ejecta of Type Ia supernovae are not consistent with pure deflagration models but are also not simply explained by delayed-detonation models. This remains a key challenge to models of thermonuclear explosions.
3. SN 1987A shows all the features displayed by core-collapse supernovae, including strongly directed flow, but also significant evidence for nonaxisymmetric structure. SN 1987A is worthy of in-depth reconsideration in the current context.

4. Spectropolarimetry of supernovae can reveal information about the properties of the interstellar dust in the host galaxy. Current data suggest that this dust frequently has properties different than dust in the Galaxy.
5. Data on stripped-core supernovae that best reveal the inner machine of core collapse need to be expanded so that statistical properties can be quantified.
6. The sample of Type Ia supernovae of all subtypes needs to be expanded to study statistical properties.
7. Quantitative, physics-based radiative transfer modeling of the full diversity of supernova spectropolarimetry is needed.

DISCLOSURE STATEMENT

J.C.W. received funding from the National Science Foundation to undertake research on the topic of this review.

ACKNOWLEDGMENTS

The authors are grateful to their fellow members of the VLT spectropolarimetry team for much of the hard work and insight that made this review possible: PI Dietrich Baade, Peter Höflich, Nando Patat, Alejandro Clocchiatti, and Justyn Maund. We give special thanks to Peter Höflich for his modeling work and early support of the Texas spectropolarimetry program when it was first getting off the ground. J.C.W. is also especially grateful to Justyn Maund for extensive and insightful discussions of supernova polarimetry and related topics and for his help with some of the graphics used here. We also thank Doug Leonard for helpful discussions and for providing specially crafted figures representing his work and Dan Kasen for comments and a key figure. We are indebted to the European Southern Observatory for the generous allocation of observing time for our VLT program and to The Paranal Science Operations staff and the User Support Group in Garching, who have gone to considerable effort to implement our demanding program. We recognize that accommodating target-of-opportunity observations in an already busy observing and work schedule often poses a special challenge. This work was supported in part by NSF Grant AST 0709181 to L.W. and NASA Grant NNG04GL00G and NSF Grant AST 0707769 to J.C.W.

LITERATURE CITED

Akiyama S, Wheeler JC, Meier DL, Lichtenstadt I. 2003. *Ap. J.* 584:954
Arnett WD, Bahcall JN, Kirshner RP, Woosley SE. 1989. *Annu. Rev. Astron. Astrophys.* 27:629
Barrett P. 1988. *MNRAS* 234:937
Benetti S, Cappellaro E, Mazzali PA, Turatto M, Altavilla G, et al. 2005. *Ap. J.* 623:1011
Benetti S, Meikle P, Stehle M, Altavilla G, Desidera S, et al. 2004. *MNRAS* 348:261
Blondin JM, Mezzacappa A. 2007. *Nature* 445:58
Boisseau JR, Wheeler JC, Oran ES, Khokhlov AM. 1996. *Ap. J. Lett.* 471:L99
Branch D, Dang LC, Hall N, Ketchum W, Melakayil M, et al. 2006. *Publ. Astron. Soc. Pac.* 118:560
Burrows A, Dessart L, Livne E, Ott CD, Murphy J. 2007. *Ap. J.* 664:416
Barrows A, Livne E, Dessart L, Ott CD, Murphy J. 2006. *Ap. J.* 640:878
Burrows CJ, Krist J, Hester JJ, Sahai R, Trauger JT, et al. 1995. *Ap. J.* 452:680
Chandrasekhar S. *Principles of Stellar Dynamics*. 1960. New York: Dover

Chieffi A, Domínguez I, Höflich P, Limongi M, Straniero O. 2003. *MNRAS* 345:111
Chornock R, Filippenko AV, Branch D, Foley RJ, Jha S, Li W. 2006. *Publ. Astron. Soc. Pac.* 118:722
Chornock R, Filippenko AV. 2006. astro-ph/0609405
Chugai NN. 1992. *Sov. Astron. Lett.* 18:168
Chugai NN. 2001. *MNRAS* 326:1448
Chugai NN. 2006. *Astron. Lett.* 32:739
Chugai NN, Chevalier RA. 2007. *Ap. J.* 657:378
Chugai NN, Fabrika SN, Sholukhova ON, Goranskij VP, Abolmasov PK, Vlasyuk VV. 2005. *Astron. Lett.* 31:792
Clocchiatti A, Marraco HG. 1988. *Astron. Astrophys.* 197:L1
Cropper M, Bailey J, McCowage J, Cannon RD, Couch WJ, et al. 1988. *MNRAS* 231:695
Crotts APS, Kunkel WE, McCarthy PJ. 1989. *Ap. J. Lett.* 347:L61
del Toro Iniesta JC. 2003. *Introduction to Spectropolarimetry*. Cambridge: Cambridge Univ. Press
Doroshenko VT, Efimov YS, Shakhovskoi NM. 1995. *Astron. Lett.* 21:513
Dotani T, Hayashida K, Inoue H, Itoh M, Koyama K. 1987. *Nature* 330:230
Fesen RA. 2001. *Ap. J. Suppl.* 133:161
Filippenko AV. 1997. *Annu. Rev. Astron. Astrophys.* 35:309
Folatelli G, Contreras C, Phillips MM, Woosley SE, Blinnikov S, et al. 2006. *Ap. J.* 641:1039
Gamezo VN, Khokhlov AM, Oran ES. 2004. *Phys. Rev. Lett.* 92:211102
Gamezo VN, Khokhlov AM, Oran ES, Chtchelkanova AY, Rosenberg RO. 2003. *Science* 299:77
Gamezo VN, Wheeler JC, Khokhlov AM, Oran ES. 1999. *Ap. J.* 512:827
Gerardy CL, Höflich P, Fesen RA, Marion GH, Nomoto K, et al. 2004. *Ap. J.* 607:391
Goodrich RW. 1991. *Publ. Astron. Soc. Pac.* 103:1314
Gorosabel J, Larionov V, Castro-Tirado AJ, Guziy S, Larionova L, et al. 2006. *Astron. Astrophys.* 459:L33
Hamuy M, Phillips MM, Suntzeff NB, Maza J, González LE, et al. 2003. *Nature* 424:651
Harkness RP, Wheeler JC. 1990. In *Supernovae*, ed. A Petschek, p. 1. New York: Springer
Hatano K, Branch D, Fisher A, Baron E, Filippenko AV. 1999. *Ap. J.* 525:881
Hillebrandt W, Niemeyer JC. 2000. *Annu. Rev. Astron. Astrophys.* 38:191
Hoffman JL, Leonard DC, Chornock R, Filippenko AV, Barth AJ, Matheson T. 2007. Preprint (arXiv:0709.3258)
Höflich P. 1991. *Astron. Astrophys.* 246:481
Höflich P. 1995. *Ap. J.* 440:821
Höflich P. 2005. *Ap. Space Sci.* 298:87
Höflich P, Gerardy CL, Marion H, Quimby R. 2006. *New Astron. Rev.* 50:470
Höflich P, Khokhlov A, Wang L. 2001. In *Proc. 20th Texas Symp. Relativ. Astrophys.*, ed. JC Wheeler, H Martel, p. 459. New York: AIP
Höflich P, Wheeler JC, Hines DC, Trammell SR. 1996. *Ap. J.* 459:307
Höflich P, Wheeler JC, Wang L. 1999. *Ap. J.* 521:179
Hough JH, Bailey JA, Rouse MF, Whittet DCB. 1987. *MNRAS* 227:1P
Howell DA, Höflich P, Wang L, Wheeler JC. 2001. *Ap. J.* 556:302
Hwang U, Laming JM, Badenes C, Berendse F, Blondin J, et al. 2004. *Ap. J. Lett.* 615:L117
Jeffery DJ. 1987. *Nature* 329:419
Jeffrey DJ. 1989. *Ap. J. Suppl.* 71:951
Jeffery DJ. 1990. *Ap. J.* 352:267
Jeffery DJ. 1991a. *Ap. J.* 375:264
Jeffery DJ. 1991b. *Ap. J. Suppl.* 77:405
Jha S, Branch D, Chornock R, Foley RJ, Li W, et al. 2006. *Ap. J.* 132:189
Kasen D, Nugent P, Thomas RC, Wang L. 2004. *Ap. J.* 610:876
Kasen D, Nugent P, Wang L, Howell DA, Wheeler JC, et al. 2003. *Ap. J.* 593:788
Kasen D, Plewa T. 2007. *Ap. J.* 662:459
Kasen D, Thomas RC, Nugent P. 2006. *Ap. J.* 651:366
Kawabata KS, Deng J, Wang L, Mazzali P, Nomoto K, et al. 2003. *Ap. J. Lett.* 593:L19
Kawabata KS, Jeffery DJ, Iye M, Ohyama Y, Kosugi G, et al. 2002. *Ap. J. Lett.* 580:L39

Khokhlov AM. 1991. *Astron. Astrophys.* 245:114
Khokhlov AM, Höflich P. 2001. In *AIP Conf. Proc. No. 556, Explos. Phenom. Astrophys. Compact Objects*, ed. H-Y Chang, C-H Lee, M Rho, p. 301. New York: AIP
Khokhlov AM, Höflich PA, Oran ES, Wheeler JC, Wang L, Chtchelkanova AY. 1999. *Ap. J. Lett.* 524:L107
Kifonidis K, Plewa T, Scheck L, Janka H-T, Müller E. 2006. *Astron. Astrophys.* 453:661
Komissarov SS, Barkov MV. 2007. *MNRAS* 382:1029
Kotake K, Sawai H, Yamada S, Sato K. 2004. *Ap. J.* 608:391
Lee TA, Wamsteker W, Wisniewski WZ, Wdowiak TJ. 1972. *Ap. J. Lett.* 177:L59
Leonard DC, Filippenko AV. 2001. *Publ. Astron. Soc. Pac.* 113:920
Leonard DC, Filippenko AV. 2005. In *ASP Conf. Ser. Proc., Supernovae Cosmol. Lighthouses*, ed. MM Turatto, S Benetti, L Zampieri, W Shea, p. 342:330. San Francisco: ASP
Leonard DC, Filippenko AV, Ardila DR, Brotherton MS. 2001. *Ap. J.* 553:861
Leonard DC, Filippenko AV, Barth AJ, Matheson T. 2000. *Ap. J.* 536:239
Leonard DC, Filippenko AV, Chornock R, Foley RJ. 2002a. *Publ. Astron. Soc. Pap.* 114:1333
Leonard DC, Filippenko AV, Ganeshalingam M, Serduke FJD, Li W, et al. 2006. *Nature* 440:505
Leonard DC, Filippenko AV, Li W, Matheson T, Kirshner RP, et al. 2002b. *Astron. J.* 124:2490
Leonard DC, Filippenko AV, Matheson T. 2000. *Am. Inst. Phys. Conf. Ser.* 522:165
Leonard DC, Li W, Filippenko AV, Foley RJ, Chornock R. 2005. *Ap. J.* 632:450
Li W, Filippenko AV, Chornock R, Berger E, Berlind P, et al. 2003. *Publ. Astron. Soc. Pap.* 115:453
Livne E. 1993. *Ap. J.* 406:L17
Livne E. 1999. *Ap. J.* 527:L97
Livne E, Asida SM, Höflich P. 2005. *Ap. J.* 632:443
Lyne AG, Lorimer DR. 1994. *Nature* 369:127
MacFadyen AI, Woosley SE. 1999. *Ap. J.* 524:262
Maeda K, Nakamura T, Nomoto K, Mazzali PA, Patat F, Hachisu I. 2002. *Ap. J.* 565:405
Maeda K, Nomoto K. 2003. *Ap. J.* 598:1163
Marietta E, Burrows A, Fryxell B. 2000. *Ap. J. Suppl.* 128:615
Masada Y, Sano T, Takabe H. 2006. *Ap. J.* 641:447
Maund JR. 2008. *Astron. Astrophys.* 418:913
Maund JR, Smartt SJ, Kudritzky RP, Podsiadlowski, Gilmore GF. 2004. *Nature* 427:129
Maund JR, Wheeler JC, Patat F, Baade D, Wang L, Höflich P. 2007a. *Astron. Astrophys.* 475:L1
Maund JR, Wheeler JC, Patat F, Baade D, Wang L, Höflich P. 2007b. *MNRAS* 381:201
Maund JR, Wheeler JC, Patat F, Wang L, Baade D, Höflich PA. 2007c. *Ap. J.* 671:1944
Maund JR, Wheeler JC, Patat F, Wang L, Baade D, Höflich PA. 2008. In preparation for *Ap. J.*
Mazzali PA, Benetti S, Altavilla G, Blanc G, Cappellaro E, et al. 2005. *Ap. J. Lett.* 623:L37
Mazzali PA, Foley RJ, Deng J, Patat F, Pian E, et al. 2007. *Ap. J.* 661:892
McCall ML. 1984. *MNRAS* 210:829
McCall ML. 1985. In *Supernovae as Distance Indicators*. Lect. Notes Phys. Vol. 224, ed. N Bartel, p. 48. Berlin: Springer
McCall ML, Reid N, Bessell MS, Wickramasinghe D. 1984. *MNRAS* 210:839
McCray R. 1993. *Annu. Rev. Astron. Astrophys.* 31:175
Meikle WPS, Matcher SJ, Morgan BL. 1987. *Nature* 329:608
Méndez M, Clocchiatti A, Benvenuto OG, Feinstein C, Marraco HG. 1988. *Ap. J.* 334:295
Miller JS, Goodrich RW. 1990. *Ap. J.* 355:456
Moiseenko SG, Bisnovatyi-Kogan GS. 2007. *Ap. Space Sci.* 311:191
Nisenson P, Papaliolios C. 1999. *Ap. J.* 518:L29
Obergaulinger M, Aloy MA, Dimmelmeier H, Müller E. 2006. *Astron. Astrophys.* 457:20
Parrent J, Branch D, Troxel MA, Casebeer D, Jeffery DJ, et al. 2007. *Publ. Astron. Soc. Pac.* 119:135
Patat F, Cappellaro E, Danziger J, Mazzali PA, Sollerman J, et al. 2001. *Ap. J.* 555:900
Patat F, Chandra P, Chevalier R, Justham S, Podsiadlowski Ph, et al. 2007. *Science* 317:924
Patat F, Romaniello M. 2006. *Publ. Astron. Soc. Pac.* 118:146
Phillips MM. 1993. *Ap. J. Lett.* 413:L105
Phillips MM, Li W, Frieman JA, Blinnikov SI, DePoy D, et al. 2007. *Publ. Astron. Soc. Pac.* 119:360

Plewa T. 2007. *Ap. J.* 657:942
Plewa T, Calder AC, Lamb DQ. 2004. *Ap. J.* 612:L37
Reinecke M, Hillebrandt W, Niemeyer JC. 2002. *Astron. Astrophys.* 391:1167
Röpke FK, Hillebrandt W, Schmidt W, Niemeyer JC, Blinnikov SI, Mazzali PA. 2007. *Ap. J.* 668:1132
Röpke FK, Woosley SE, Hillebrandt W. 2007. *Ap. J.* 660:1344
Schlegel EM. 1990. *MNRAS* 244:269
Schwarz HE, Mundt R. 1987. *Astron. Astrophys.* 177:L4
Serkowski K. 1970. *Ap. J.* 160:1083
Serkowski K, Mathewson DL, Ford VL. 1975. *Ap. J.* 196:261
Shakhovskoi NM. 1976. *Sov. Astron. Lett.* 2:107
Shakhovskoi NM, Efimov YS. 1972. *Sov. Astron.* 16:7
Shapiro PR, Sutherland PG. 1982. *Ap. J.* 263:902
Shibata M, Karino S, Eriguchi Y. 2003. *MNRAS* 343:619
Simmons JFL, Stewart BG. 1985. *Astron. Astrophys.* 142:100
Spyromilio J, Bailey J. 1993. *Proc. Astron. Soc. Aust.* 10:263
Swartz DA, Filippenko AV, Nomoto K, Wheeler JC. 1993. *Ap. J.* 411:313
Thompson TA, Chang P, Quataert E. 2004. *Ap. J.* 611:380
Tominaga N, Tanaka M, Nomoto K, Mazzali PA, Deng J, et al. 2005. *Ap. J. Lett.* 633:L97
Trammell SR, Hines DC, Wheeler JC. 1993. *Ap. J. Lett.* 414:L21
Tran HD, Filippenko AV, Schmidt GD, Bjorkman KS, Jannuzi BT, Smith PS. 1997. *Proc. Astron. Soc. Pac.* 109:489
Travaglio C, Hillebrandt W, Reinecke M, Thielemann F-K. 2004. *Astron. Astrophys.* 425:1029
Uzdensky DA, MacFadyen AI. 2007. *Ap. J.* 669:546
van de Hulst HC. 1957. *Light Scattering by Small Particles*. New York: Wiley
van Paradijs J, Kouveliotou C, Wijers RAMJ. 2000. *Annu. Rev. Astron. Astrophys.* 38:37
Wampler EJ, Wang L, Baade D, Banse K, D'Odorico S, et al. 1990. *Ap. J. Lett.* 362:L13
Wang L. 2005. *Ap. J. Lett.* 635:L1
Wang L, Baade D, Höflich P, Khokhlov A, Wheeler JC, et al. 2003a. *Ap. J.* 591:1110
Wang L, Baade D, Höflich P, Wheeler JC. 2002b. *ESO Messenger* 109:47
Wang L, Baade D, Höflich P, Wheeler JC. 2003b. *Ap. J.* 592:457
Wang L, Baade D, Höflich P, Wheeler JC, Kawabata K, et al. 2006. *Ap. J.* 653:490
Wang L, Baade D, Höflich P, Wheeler JC, Kawabata K, Nomoto K. 2004. *Ap. J.* 604:L53
Wang L, Baade D, Patat F. 2007. *Science* 315:212
Wang L, Howell DA, Höflich P, Wheeler JC. 2001. *Ap. J.* 550:1030
Wang L, Wheeler JC. 1996. *Ap. J. Lett.* 462:L27
Wang L, Wheeler JC. 1998. *Ap. J. Lett.* 504:L87
Wang L, Wheeler JC, Höflich P. 1997. *Ap. J. Lett.* 476:L27
Wang L, Wheeler JC, Höflich P, Khokhlov A, Baade D, et al. 2002a. *Ap. J.* 579:671
Wang L, Wheeler JC, Li Z, Clocchiatti A. 1996. *Ap. J.* 467:435
Wheeler JC. 2000. *Am. Ins. Phys. Conf. Ser.* 522:445
Wheeler JC, Filippenko AV. 1996. *IAU Colloq. 145: Supernovae and Supernova Remnants*, ed. R McCray, Z Wang, p. 241. Cambridge: Cambridge Univ. Press
Wheeler JC, Maund JR, Couch SM. 2008. *Ap. J.* 677:1091
Wheeler JC, Meier DL, Wilson JR. 2002. *Ap. J.* 568:807
Wheeler JC, Yi I, Höflich P, Wang L. 2000. *Ap. J.* 537:810
Whittet DCB, Martin PG, Hough JH, Rouse MF, Bailey JA, Axon DJ. 1992. *Ap. J.* 386:562
Wolstencroft RD, Kemp JC. 1972. *Nature* 238:452
Wood R, Andrews PJ. 1974. *MNRAS* 167:13
Woosley SE, Bloom JS. 2006. *Annu. Rev. Astron. Astrophys.* 44:507
Yamada S, Sawai H. 2004. *Ap. J.* 608:907

Annual Review of Astronomy and Astrophysics

Volume 46, 2008

Contents

A Serendipitous Journey
Alexander Dalgarno 1

The Growth Mechanisms of Macroscopic Bodies in Protoplanetary Disks
Jürgen Blum and Gerhard Wurm 21

Water in the Solar System
Thérèse Encrenaz 57

Supernova Remnants at High Energy
Stephen P. Reynolds 89

The Crab Nebula: An Astrophysical Chimera
J. Jeff Hester 127

Pulsating White Dwarf Stars and Precision Asteroseismology
D.E. Winget and S.O. Kepler 157

The *Spitzer* View of the Extragalactic Universe
Baruch T. Soifer, George Helou, and Michael Werner 201

Neutron-Capture Elements in the Early Galaxy
Christopher Sneden, John J. Cowan, and Roberto Gallino 241

Interstellar Polycyclic Aromatic Hydrocarbon Molecules
A.G.G.M. Tielens 289

Evolution of Debris Disks
Mark C. Wyatt 339

Dark Energy and the Accelerating Universe
Joshua A. Frieman, Michael S. Turner, and Dragan Huterer 385

Spectropolarimetry of Supernovae
Lifan Wang and J. Craig Wheeler 433

Nuclear Activity in Nearby Galaxies
Luis C. Ho 475

The Double Pulsar
M. Kramer and I.H. Stairs 541

Indexes

Cumulative Index of Contributing Authors, Volumes 35–46 573

Cumulative Index of Chapter Titles, Volumes 35–46 576

Errata

An online log of corrections to *Annual Review of Astronomy and Astrophysics* articles may be found at http://astro.annualreviews.org/errata.shtml